

**Supporting information for**  
**Heterotrimetallic ring opening copolymerisation catalysis: Structure-activity**  
**relationships**

Alex Plajer, Charlotte K Williams\*

Oxford Chemistry, Chemical Research Laboratory, 12 Mansfield Road, Oxford, OX1  
3TA, UK; \*charlotte.williams@chem.ox.ac.uk,

## Contents

Section S1: Methods .....	3
Section S2: Summary of ROCOP results and comparison to previous reports .....	5
Section S3: Synthesis and Characterisation of $H_2L^2$ and $2_{ZnNa}$ and Polymerisation kinetics of $2_{ZnNa}$ .....	9
Section S4: Synthesis and Characterisation of $H_2L^3$ and $3_{ZnNa}$ and Polymerisation kinetics of $3_{ZnNa}$ .....	15
Section S5: Synthesis and Characterisation of $H_2L^4$ and $4_{ZnNa}$ and Polymerisation kinetics of $4_{ZnNa}$ .....	22
Section S6: Synthesis and Characterisation of $H_2L^5$ and $5_{ZnNa}$ and Polymerisation kinetics of $5_{ZnNa}$ .....	28
Section S7: Synthesis and Characterisation of $H_2L^6$ and $6_{ZnNa}$ and Polymerisation kinetics of $6_{ZnNa}$ .....	35
Section S8: Synthesis, characterisation and polymerisation kinetics of $1_{MgNa}$ .....	40
Section S9: Synthesis, characterisation and polymerisation kinetics of $1_{NiNa}$ .....	45
Section S10: Synthesis, characterisation and polymerisation kinetics of $1_{AlNa}$ .....	48
Section S11: Synthesis, characterisation and polymerisation kinetics of $1_{CoNa}$ .....	51
Section S12 Bibliography .....	53

## Section S1: Methods

**Materials:** Solvents and reagents were obtained from commercial sources and used as received unless stated otherwise. Cyclohexene oxide was dried over calcium hydride overnight and purified via fractional distillation prior to use and stored in an inert atmosphere. Phthalic anhydride was extracted with dry benzene, recrystallised from dry chloroform and sublimed at 100 °C and 0.05 bar. Commercial 1,2-cyclohexenediol was recrystallized from dry chloroform and dried under dynamic vacuum before use. 99.8% carbon dioxide supplied by BOC Ltd was dried by passing it through two drying columns (VICI Metronics carbon dioxide purifier) prior to use. **A**, **H<sub>2</sub>L<sub>1</sub>** and **1<sub>Co</sub>** were synthesized according to procedures published by *Akine* and coworkers.<sup>[1,2]</sup>

NMR spectra were recorded on a Bruker Avance 200 QNP or Bruker Avance 500 MHz cryo spectrometer. All spectra were recorded with external standards. Unambiguous assignments of NMR resonances were made on the basis of 2D NMR experiments.

UV-visible spectra were collected on a Varian Cary 50 UV spectrometer.

Gel permeation chromatography analysis was carried out on a Shimadzu LC-20AD instrument equipped with two mixed bed PSS SDV linear S columns in series, THF as the eluent at a flow rate of 1mL/min and at 40 °C. Polymer molecular mass ( $M_n$ ) was determined by comparison against narrow molecular mass polystyrene standards which were used to calibrate the instrument. Each polymer sample was dissolved in HPLC-grade THF (10 mg/mL) and filtered through a 0.20 µm porous filter frit prior to analysis.

High-resolution ESI mass spectra were obtained using a Thermofisher LTQ Orbitrap XL, by the EPSRC UK National Mass Spectrometry Facility at Swansea University.

Elemental analysis was obtained using a Perkin Elmer 240 Elemental Analyser, by Dr Nigel Howard from the elemental analysis lab at the University of Cambridge.

**General Polymerization protocols:** A mixture of the catalyst (5.0 µmol, 1 equiv.), 1,2-cyclohexenediol (11.7 mg, 100.0 µmol, 20 equiv.), phthalic anhydride (if used, 148.7 mg, 1.0 mmol, 200 equiv.) and cyclohexene oxide (2 mL, 20.0 mmol, 4000 equiv.) was added to a Schlenk tube, under nitrogen. If carbon dioxide was applied, the reaction was subjected to three vacuum/CO<sub>2</sub> cycles (pressure regulated at 1 bar CO<sub>2</sub>). If carbon dioxide was not used, the Schlenk tube was connected to vacuum/nitrogen line. The Schlenk tube was fitted with a DiComp probe for *in situ*-ATRIR spectroscopy (REACTIR) and submerged into an oil bath that was preheated to the appropriate temperature. At this point the REACTIR instrument was set to begin data-collection ( $t_0$ ). After the reaction was completed, the mixture was allowed to cool to room temperature and the crude product composition was analysed by NMR spectroscopy

of an aliquot to determine the ratio of products (poly(cyclohexene carbonate) PCHC, poly(cyclohexene oxide) PCHO, poly(cyclohexene-alt-phthalate) PCHPE and cyclohexene carbonate c5c). The polymer was isolated by adding the concentrated polymerisation mixture (ca 0.5 mL, achieved by removing excess CHO under a stream of N<sub>2</sub>) to 100 mL of acidified MeOH (10 µL concentrated HCl, per 100 mL MeOH) resulting in the precipitation of the polymer.

## Section S2: Summary of ROCOP results and comparison to previous reports

Cat. <sup>a</sup>	Polymer Selectivity (%) <sup>b</sup>	Carbonate: Ether (%) <sup>c</sup>	Polymer TON <sup>d</sup>	Polymer TOF [h <sup>-1</sup> ] <sup>e</sup>	M <sub>n</sub> [kg/mol] (Đ) <sup>f</sup>
1 <sub>ZnNa</sub> <sup>g</sup>	97	86:14	1960	478	5.61 (1.29)
2 <sub>ZnNa</sub>	95	82:18	1440	416	4.65 (1.22)
3 <sub>ZnNa</sub>	97	95:5	800	310	3.01 (1.19)
4 <sub>ZnNa</sub>	95	87:13	1956	1084	5.48 (1.18)
5 <sub>ZnNa</sub>	91	78:22	1740	282	5.43 (1.23)
6 <sub>ZnNa</sub>	inactive	-	-	-	-
1 <sub>MgNa</sub>	62	>99:1	314	16	n.d.
1 <sub>AlNa</sub>	Decomp.	-	-	-	-
1 <sub>NiNa</sub>	Decomp.	-	-	-	-
1 <sub>CoNa</sub> <sup>*</sup>	>99	73:27	520	270	2.0 (1.15)

**Table S 1:** <sup>a</sup>Copolymerization conditions: 0.025 mol% catalyst loading (1:4000), 20 equiv. 1,2-cyclohexane diol (CHD), 1 bar CO<sub>2</sub>, CHO neat (9.99 M), 100°C (\*80°C). Polymerizations were stopped once conversions versus time plots deviate from linearity. <sup>b</sup>Determined by comparison of the relative integrals, in the normalised <sup>1</sup>H NMR spectrum (CDCl<sub>3</sub>, 25°C), of resonances due to polymer (δ 4.65 ppm, 3.45 ppm) and cyclic carbonate (δ 4.00 ppm). <sup>c</sup>Determined by comparison of the relative integrals, in the normalised the <sup>1</sup>H NMR spectrum, of resonances due to carbonate (δ 4.65 ppm) and ether (δ 3.45 ppm) linkages. <sup>d</sup>Turnover number (TON), number of moles of CHO consumed per mole of catalyst. <sup>e</sup>Turnover frequency (TOF) determined from initial rates analysis by *in situ* ATR-IR spectroscopy (typically 5 – 15% conversion) as TON/time. <sup>f</sup>Determined by GPC (gel permeation chromatography) measurements conducted in THF, using narrow MW polystyrene standards to calibrate the instrument; Đ = M<sub>w</sub>/M<sub>n</sub>. <sup>g</sup>According to Reference [3].

Cat. <sup>a</sup>	PE TOF [h <sup>-1</sup> ] <sup>b</sup>	PCHO TON[h <sup>-1</sup> ] <sup>c</sup>	M <sub>n</sub> [kg/mol] (Đ) <sup>d</sup>
1 <sub>ZnNa</sub> <sup>e</sup>	173	-	-
2 <sub>ZnNa</sub>	120	208	2.26 (1.18)
3 <sub>ZnNa</sub>	225	56	1.90 (1.17)
4 <sub>ZnNa</sub>	92	120	2.05 (1.16)
5 <sub>ZnNa</sub> <sup>†</sup>	6	-	1.05 (1.16)
6 <sub>ZnNa</sub>	50	-	1.75 (1.15)
1 <sub>MgNa</sub>	142	840	3.97 (1.19)
1 <sub>NiNa</sub>	Decomp.	-	-
1 <sub>AlNa</sub>	Decomp.	-	-
1 <sub>CoNa</sub> <sup>*</sup>	136, 51	200	2.23 (1.17)

**Table S 2:** <sup>a</sup>Copolymerization conditions: 0.025 mol% catalyst loading (1:4000), 20 equiv. 1,2-cyclohexane diol (CHD), 200 equiv. PA (†100 equiv.), CHO neat (9.99 M), 100°C (\*80°C). Polymerizations were stopped once CHO to PCHO conversions versus time plots deviate from linearity after complete PA consumption. <sup>b</sup>Turnover frequency (TOF) determined from rate analysis by *in situ* ATR-IR spectroscopy (typically 20 – 80% PA conversion) as TON/time. <sup>c</sup>Turnover number (TON), number of moles of CHO consumed per mole of catalyst, overall turnover determined by <sup>1</sup>H NMR. <sup>d</sup>Determined by GPC (gel permeation chromatography) measurements conducted in THF, using narrow MW polystyrene standards to calibrate the instrument; Đ = M<sub>w</sub>/M<sub>n</sub>. <sup>e</sup>According to Reference [3].

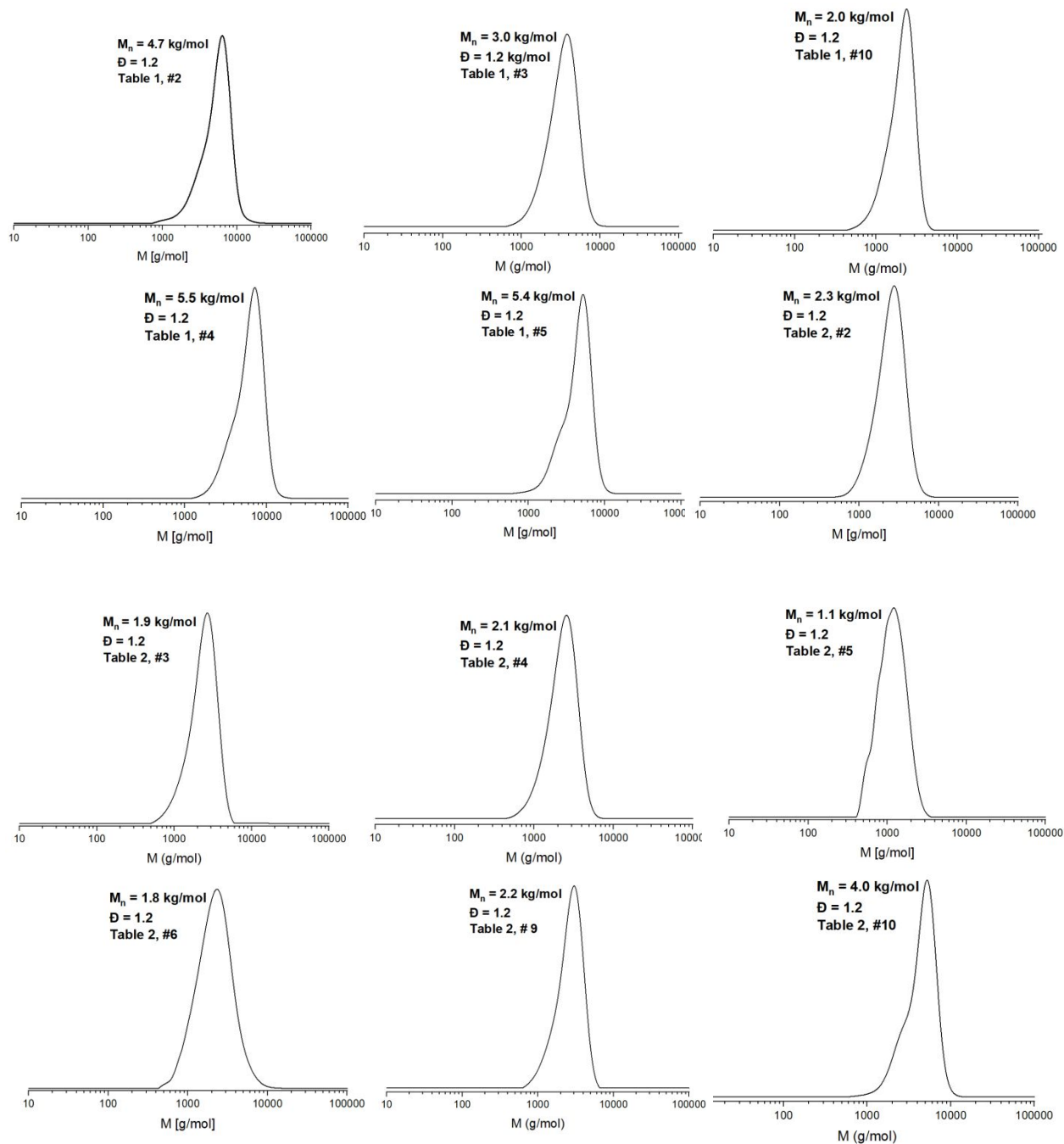
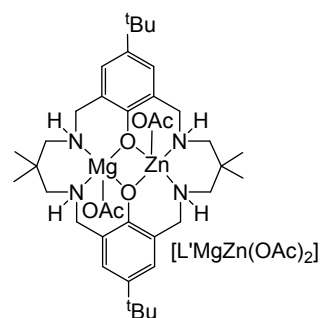
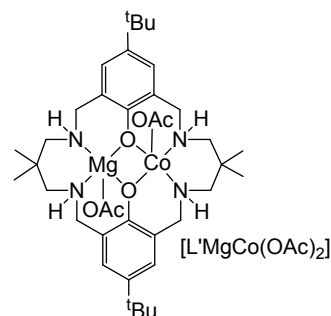


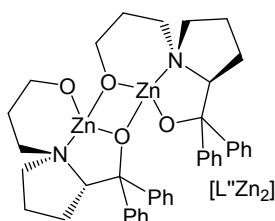
**Figure S 1:** GPC traces of polymers produced in this study.



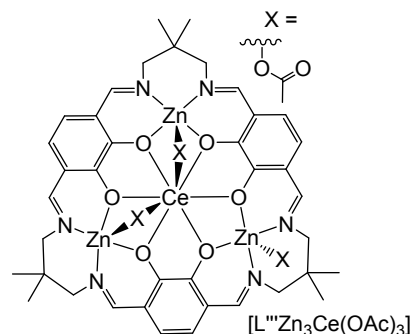
TOF 148 h<sup>-1</sup> at 100 °C, 0.05 mol%, 1 bar CO<sub>2</sub>  
>99% PCHC  
in preparation



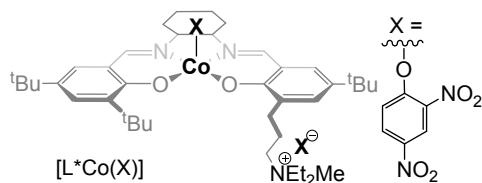
TOF 350 h<sup>-1</sup> at 100 °C, 0.05 mol%, 1 bar CO<sub>2</sub>  
>99% PCHC  
Nat. Chem., 2020, 12, 372 - 380



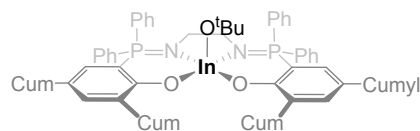
TOF 74 h<sup>-1</sup> at 80 °C, 0.07 mol%, 1 bar CO<sub>2</sub>  
>99% PCHC  
Chem. Eur. J., 2017, 23, 16472 - 16475



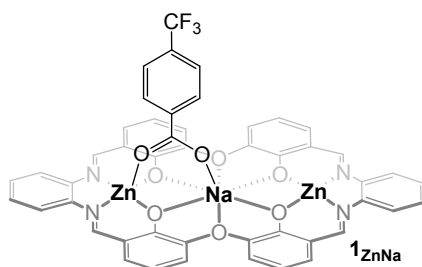
TOF 100 h<sup>-1</sup> at 100 °C, 0.05 mol%, 3 bar CO<sub>2</sub>  
>99% PCHC  
Angew. Chem. Int. Ed., 2018, 57, 2492 - 2496



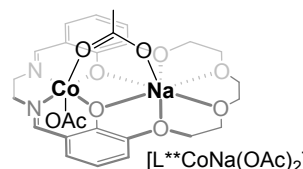
TOF 136 h<sup>-1</sup> at 50 °C, 0.02 mol%, 1 bar CO<sub>2</sub>  
>99% PCHC  
Macromolecules, 2010, 43, 1396 - 1402



TOF 15 h<sup>-1</sup> at 80 °C, 1 mol%, 1 bar CO<sub>2</sub>  
>99% PCHC  
J. Am. Chem. Soc., 2018, 140, 6893 - 1903



TOF 478 h<sup>-1</sup> at 100 °C, 0.025 mol%, 1 bar CO<sub>2</sub>  
86% PCHC, 14% PCHO  
Angew. Chem. Int. Ed., 2021, 60, 13372 - 13379



TOF 795 h<sup>-1</sup> at 100 °C, 0.025 mol%, 1 bar CO<sub>2</sub>  
>99% PCHC  
Chem. Eur. J., accepted, DOI: 10.1002/chem.202101140

**Figure S 2:** Selected high activity, under low carbon dioxide pressure (<3 atm), catalysts for CO<sub>2</sub>/CHO ROCOP. Note that the activity values are quoted per initiating group in each case.

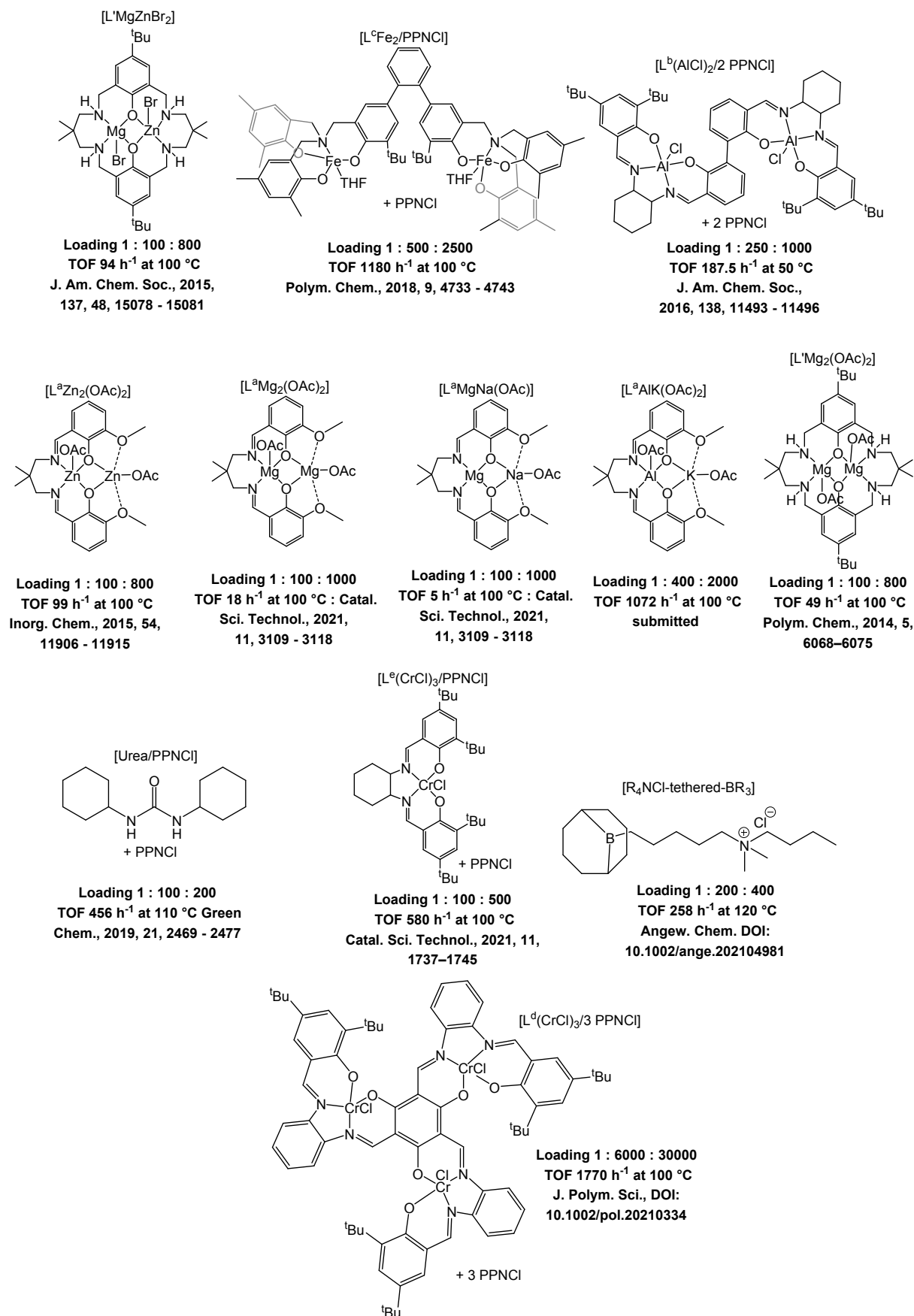
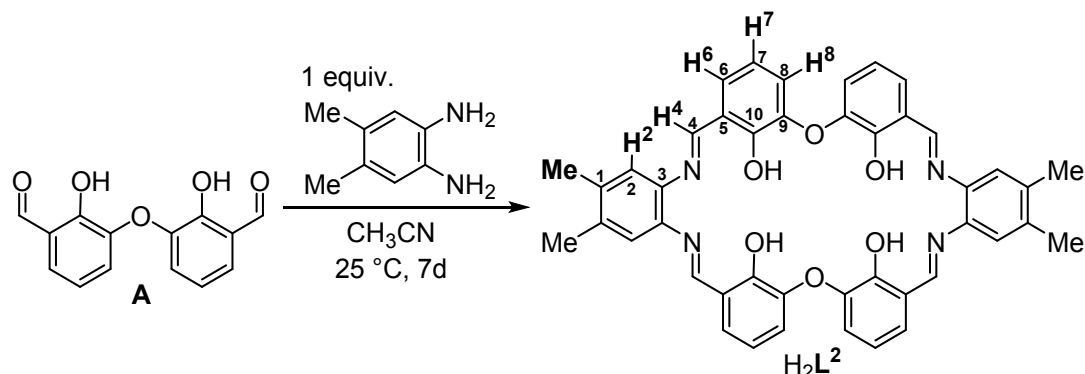


**Figure S 3:** High activity, PA/CHO ROCOP catalysts previously reported in the literature. Activity is given per initiator and the loading is reported as per catalyst : PA : CHO

**Section S3: Synthesis and Characterisation of  $H_2L^2$  and  $2_{ZnNa}$  and Polymerisation kinetics of  $2_{ZnNa}$**



**Scheme S 1:** Synthesis of  $H_2L^2$  from **A** and NMR assignment numbering for  $Zn_2Na$ .

**Synthesis of  $H_2L^2$ :** A solution of **A** (71.6 mg, 0.28 mmol, 1 equiv.) in acetonitrile (4 mL) was added to a solution of 4,5-dimethyl-phenylenediamine (37.6 mg, 0.28 mmol, 1 equiv.) in acetonitrile (4 mL). The mixture was allowed to stand for one week at room temperature during which orange crystals formed, which were isolated by decantation, washed with  $Et_2O$  (1mL) and dried *in vacuo* to yield  $H_2L^2 \cdot 1.5H_2O$  as an orange crystalline powder (32.3 mg, 43  $\mu$ mol, 31%).

**$^1H$  NMR (400 MHz,  $CDCl_3$ )**  $\delta$  13.30 (s, 1H, OH), 8.59 (s, 1H, H4), 7.12 (dd,  $J = 7.9, 1.6$  Hz, 1H, H6), 7.05 – 6.91 (m, 2H, H2, H8), 6.80 (t,  $J = 7.8$  Hz, 1H, H7), 2.33 (s, 3H, Me).

**$^{13}C\{^1H\}$  NMR (126 MHz, 1:1  $d_6$ -DMSO: $CDCl_3$ )**  $\delta$  161.73 (C4), 151.79 (C10), 143.80 (C9), 139.14 (C3), 136.37 (C1), 126.38 (C6), 121.02 (C8), 119.84 (C2), 119.34 (C5), 117.74 (C7), 18.98 (Me).

**Elemental Analysis ( $H_2L^2 \cdot 1.5H_2O$ ,  $C_{44}H_{39}N_4O_{7.5}$ )** calculated C 71.1% H 5.3% N 7.5% found C 71.0% H 5.0% N 7.4%

**HRESI-MS  $m/z$**  = calculated  $[M + H]^+$  717.2708,  $[M + Na]^+$  739.2527. Found  $[M + H]^+$  717.2709,  $[M + Na]^+$  739.2522

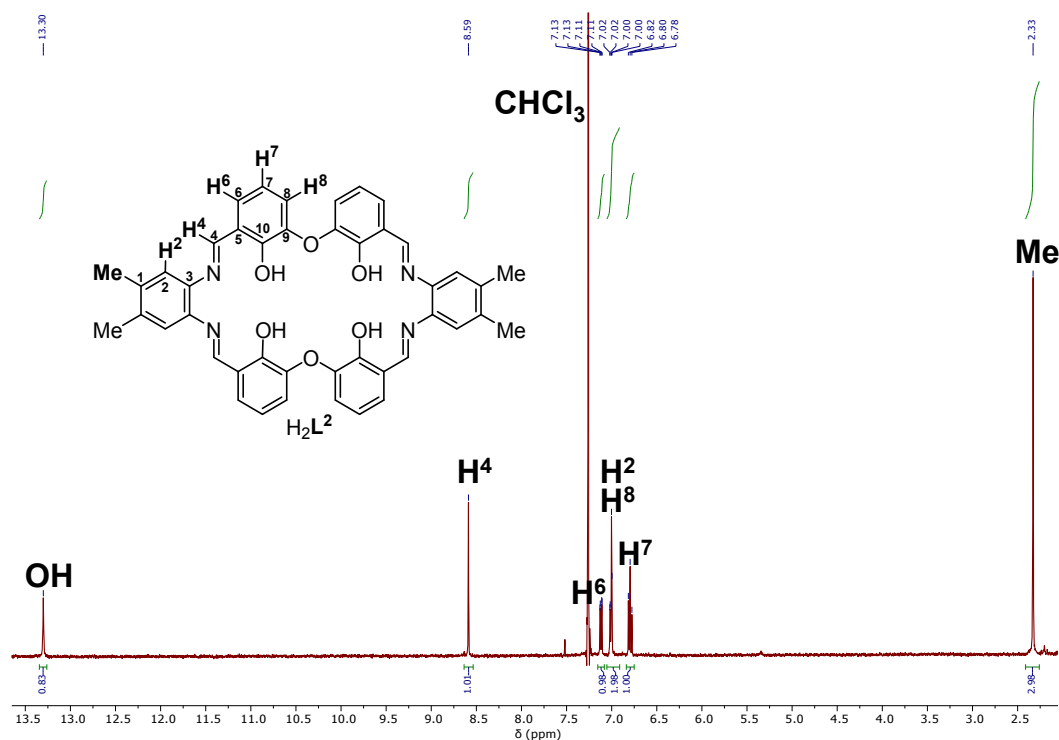


**Figure S 4:**  $^1\text{H}$  NMR spectrum (500 MHz,  $d_6$ -DMSO, 25°C) of  $\text{H}_2\text{L}^2$ .

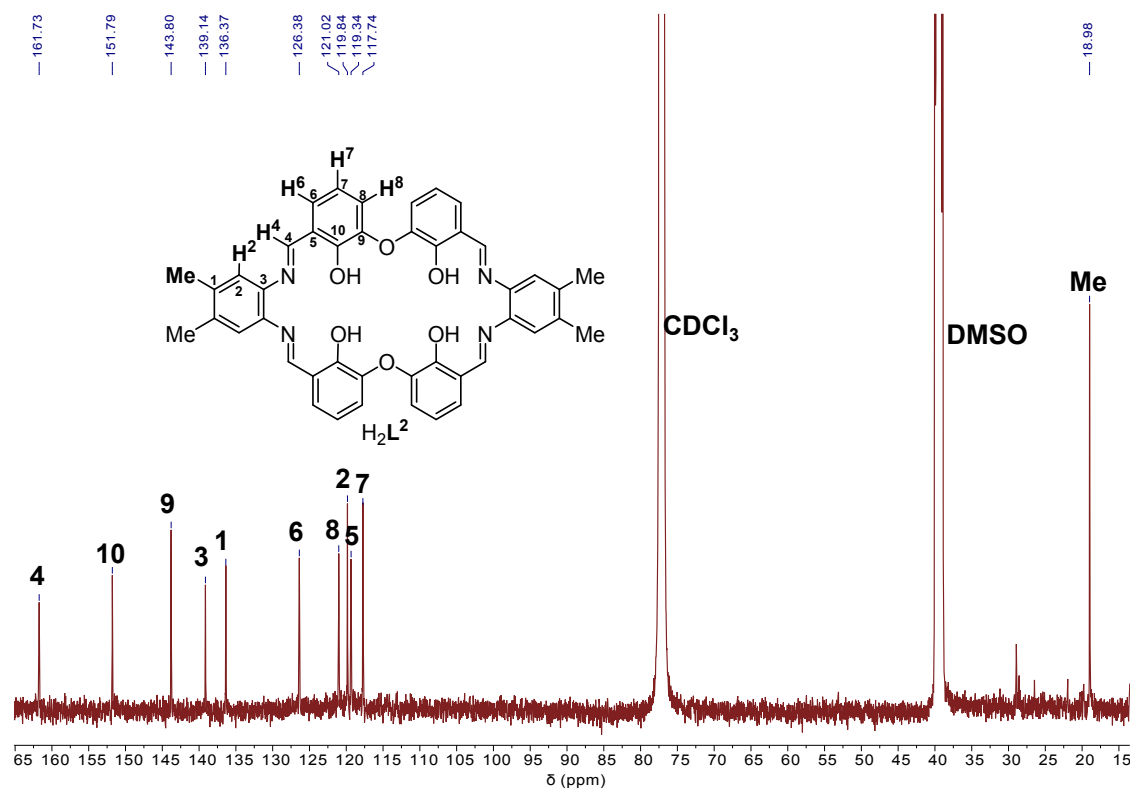


**Figure S 5:**  $^{13}\text{C}\{^1\text{H}\}$  NMR spectrum (126 MHz, 1:1  $d_6$ -DMSO: $\text{CDCl}_3$ , 25°C) of  $\text{H}_2\text{L}^2$ .

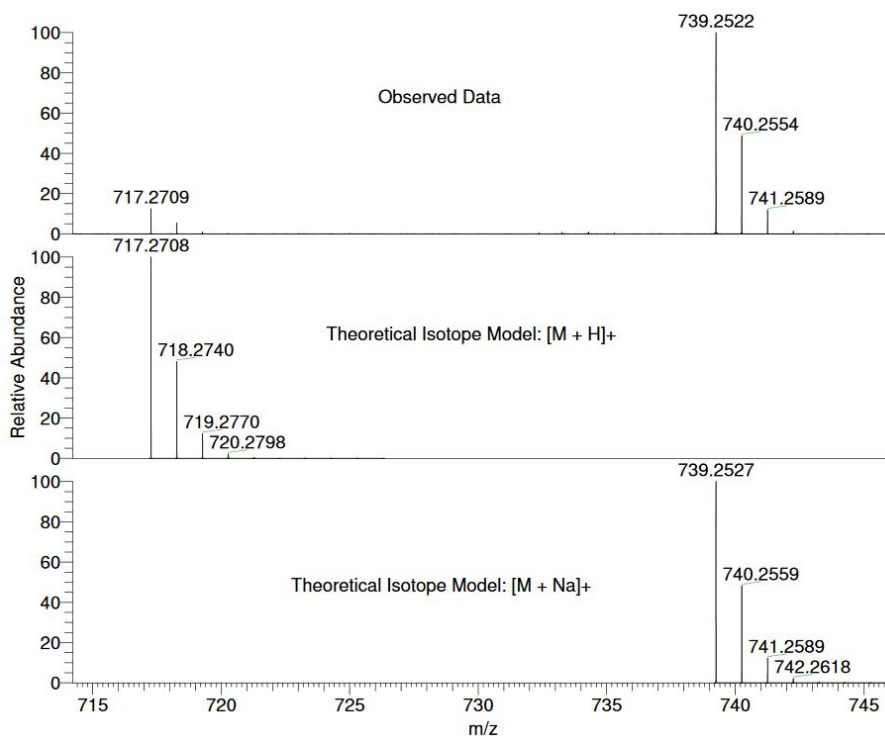
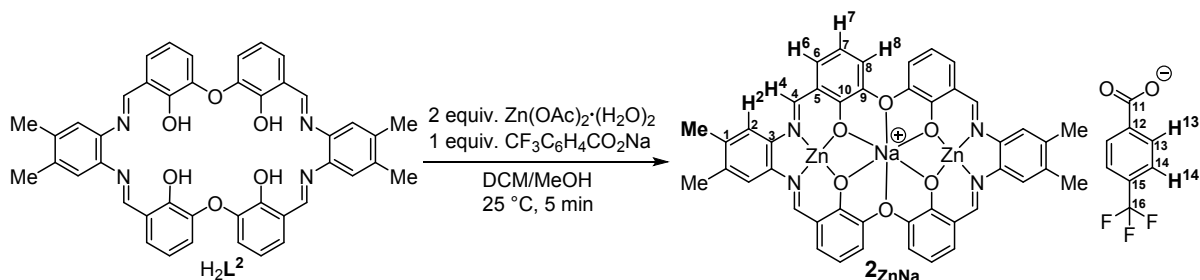


**Figure S 6:** Positive mode high-resolution ESI mass spectrum of  $H_2L^2$ .



**Scheme S 2:** Synthesis of  $2ZnNa$  from  $H_2L^2$  and NMR assignment numbering for  $2ZnNa$ .

**Synthesis of  $2ZnNa$ :** A solution of  $Zn(OAc)_2 \cdot (H_2O)_2$  (33.3 mg, 151  $\mu$ mol, 2 equiv.) and  $CF_3C_6H_4CO_2Na$  (17.2 mg, 75  $\mu$ mol, 1 equiv.) in MeOH (5 mL) was added to a solution of  $H_2L^2$  (53.8 mg, 75  $\mu$ mol, 1 equiv.) in 5 mL DCM (5 mL). The resulting solution was left unperturbed for 5 min. Afterwards all volatiles were removed *in vacuo* yielding a semi-solid which was washed with  $Et_2O$  (100 mL). To remove the acetic acid by-product fully, the crude product was suspended in toluene (20 mL) which was afterwards removed under vacuum. This process was repeated, yielding  $Zn_2Na \cdot 2.5H_2O$  as an orange powder (80 mg, 73  $\mu$ mol, 96%).

**$^1H$  NMR (500 MHz,  $d_6$ -DMSO)**  $\delta$  8.81 (s, 1H, H4), 7.92 (s, 0.5H, H13), 7.62 (s, 0.5H, H14), 7.57 (s, 1H, H2), 7.20 (d,  $J = 7.3$  Hz, 1H, H6), 7.16 (d,  $J = 7.7$  Hz, 1H, H8), 6.52 (t,  $J = 7.9$  Hz, 1H, H7), 2.33 (s, 3H, Me).

$^{13}\text{C}\{^1\text{H}\}$  NMR (126 MHz,  $d_6$ -DMSO)  $\delta$  168.36 (C11), 162.91 (C4), 162.30 (C3), 148.47 (C9), 140.94 (C12), 137.93 (C10), 136.21 (C1), 130.50 (C6), 130.12 (C13), 124.31 (q,  $J = 271$  Hz, C16), 124.46 (C14), 120.84 (C15, C5), 120.59 (C8), 117.66 (C2), 111.81 (C7), 19.49 (Me).

$^{19}\text{F}\{^1\text{H}\}$  NMR (470 MHz,  $d_6$ -DMSO)  $\delta$  -61.01.

Elemental Analysis ( $2\text{ZnNa} \cdot 2.5\text{H}_2\text{O}$ ,  $\text{C}_{52}\text{H}_{41}\text{F}_3\text{N}_4\text{O}_{10.5}\text{Zn}_2$ ) calculated C 56.8% H 3.8% N 5.1% found C 57.2% H 3.4% N 4.7%

HRESI-MS  $m/z$  = calculated  $[\text{M} - \text{CF}_3\text{C}_6\text{F}_4\text{CO}_2\text{Na}]^+$  865.0766. Found 865.0773

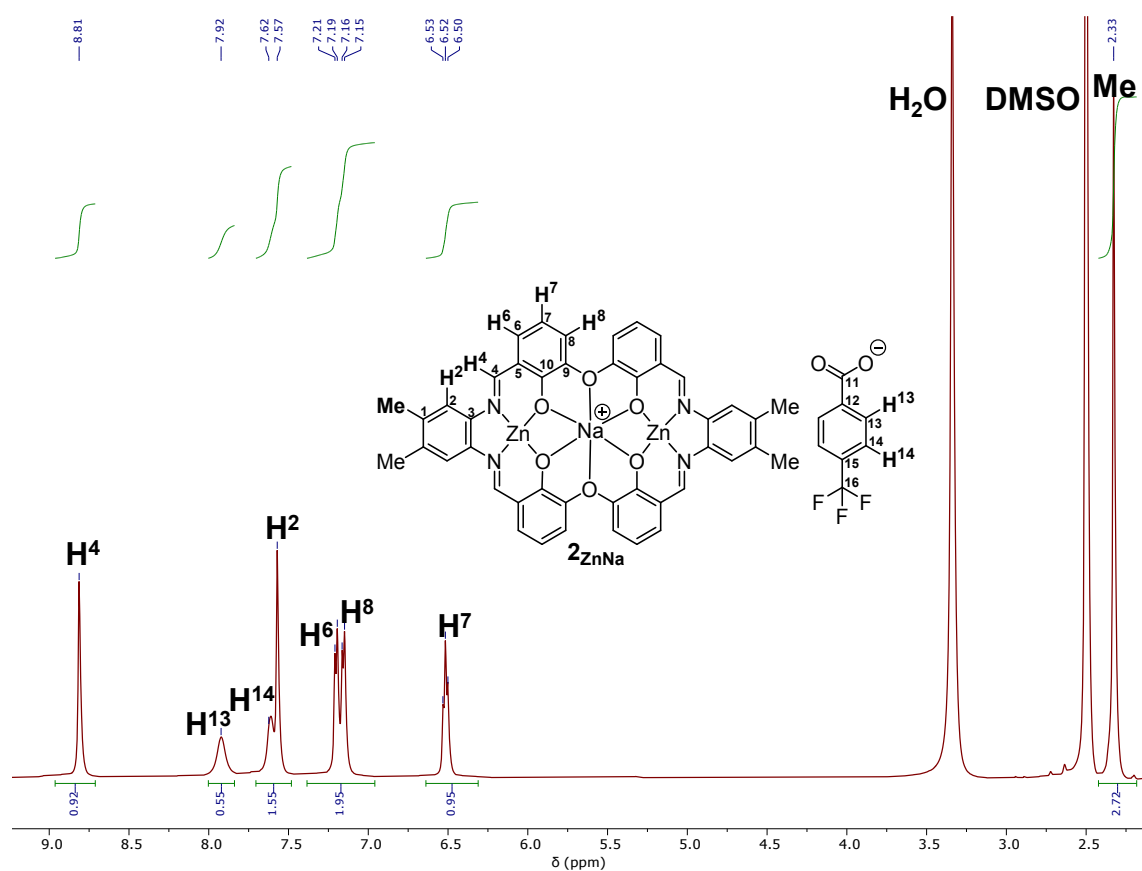
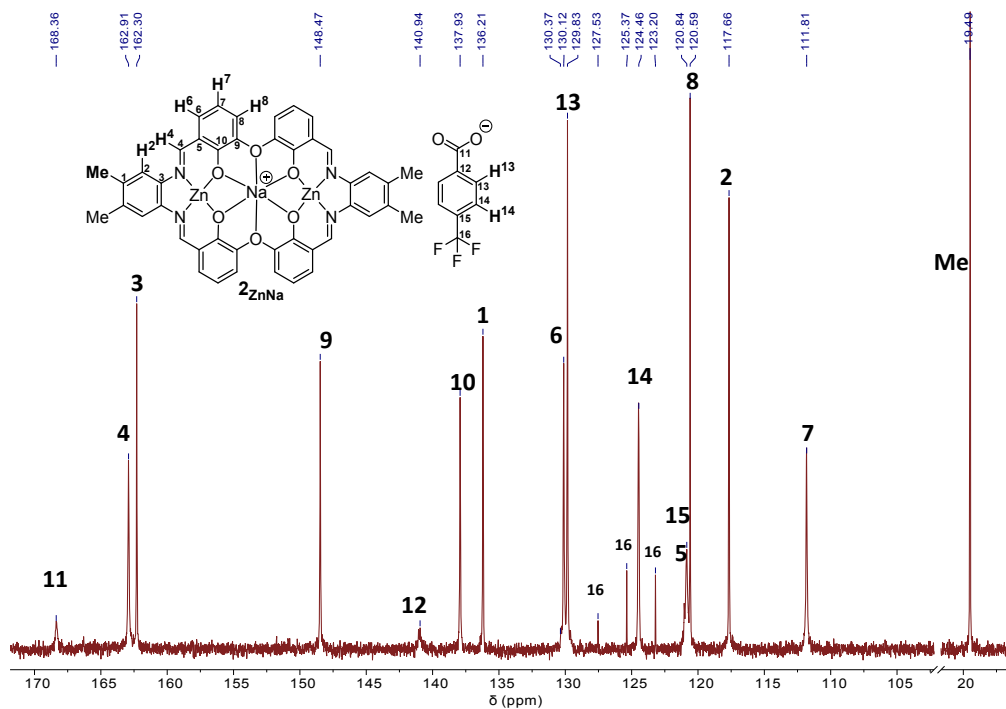
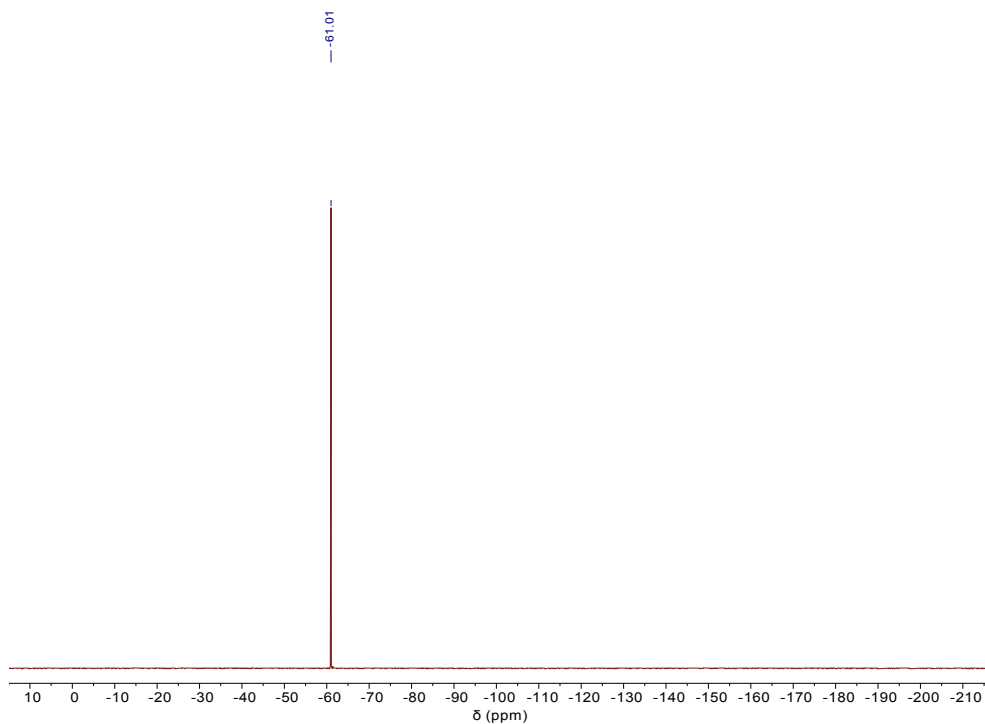


Figure S 7:  $^1\text{H}$  NMR spectrum (500 MHz,  $d_6$ -DMSO,  $25^\circ\text{C}$ ) of  $2\text{ZnNa}$ .



**Figure S 8:**  $^{13}C\{^1H\}$  NMR spectrum (126 MHz,  $d_6$ -DMSO, 25°C) of  $2_{ZnNa}$ .



**Figure S 9:**  $^{19}F\{^1H\}$  NMR (470 MHz,  $d_6$ -DMSO, 25°C) of  $2_{ZnNa}$ .

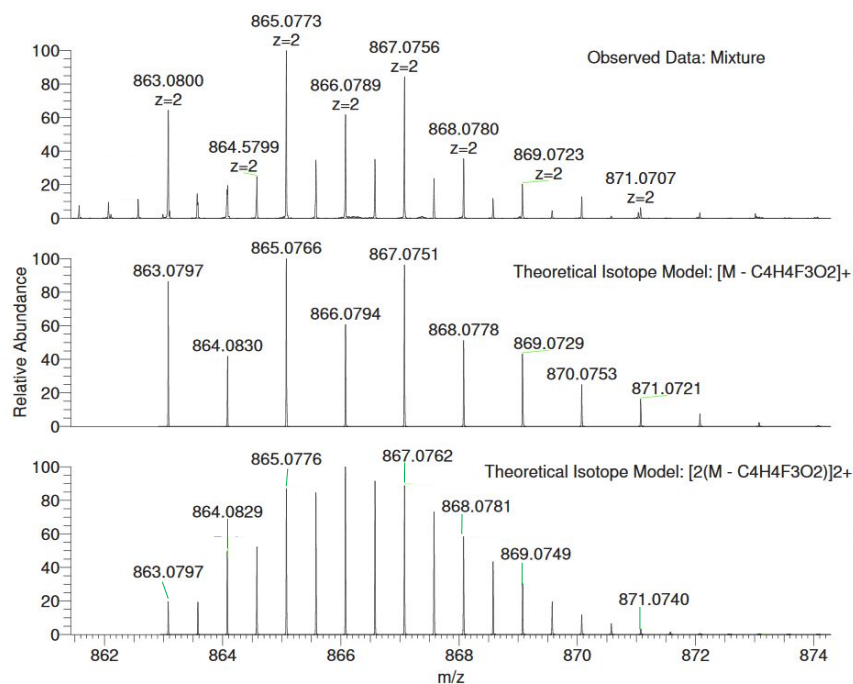


**Figure S 10:** Positive mode high-resolution ESI mass spectrum of  $2_{\text{ZnNa}}$ .

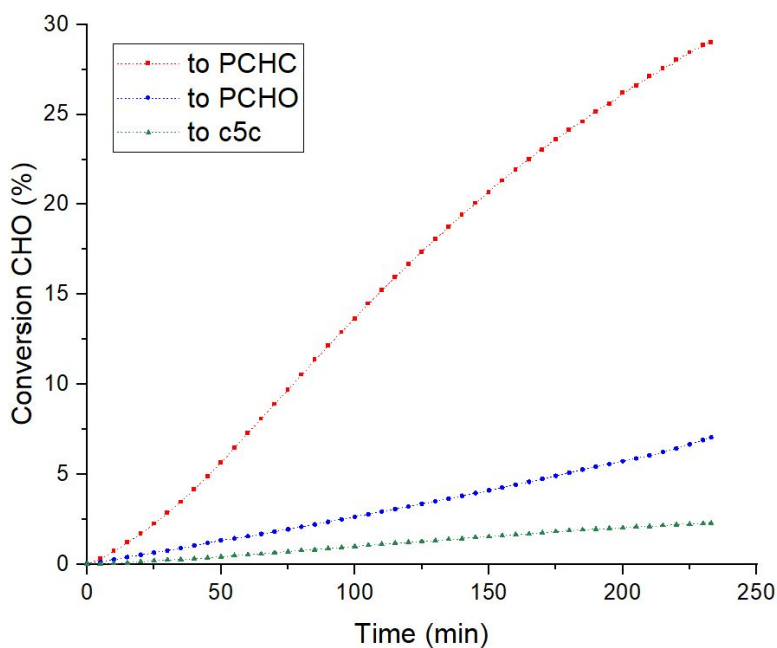


**Figure S 11:** Plot showing conversion of CHO to polymer (PCHC and PCHO) and c5c vs. time (

**Table S 1**, run #2). Data are obtained using *in situ* ATR-IR spectroscopic monitoring of polymerizations conducted using 1 equiv.  $3_{\text{ZnNa}}$ , 20 equiv. cyclohexane diol (CHD), 4000 equiv. cyclohexene oxide (CHO) and 1 bar carbon dioxide pressure at 100 °C. The conversion data was obtained by monitoring the changes to absorptions at 1744  $\text{cm}^{-1}$  (PCHC), 1089  $\text{cm}^{-1}$  (PCHO) and 1785  $\text{cm}^{-1}$  (c5c). The turn-over-frequency (TOF) were obtained from 5-15.0% conversion to PCHC.

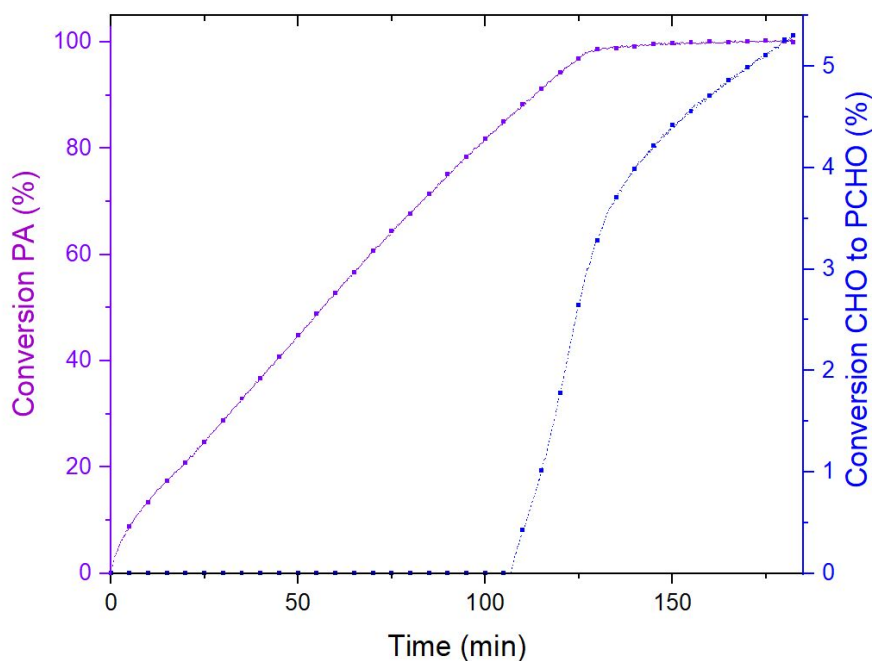
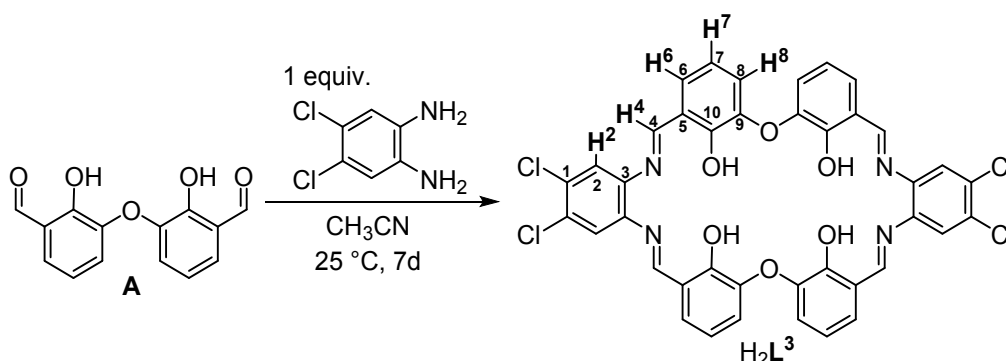


**Figure S 12:** Plot showing conversion of PA and CHO to polymer (PCHPE and PCHO respectively) vs. time (**Table S 2**, run #2). Data are obtained using *in situ* ATR-IR spectroscopic monitoring of polymerizations conducted using 1 equiv.  $\text{Zn}_2\text{Na}$ , 20 equiv. cyclohexane diol (CHD), 200 equiv PA, 4000 equiv. cyclohexene oxide (CHO) and 1 bar  $\text{N}_2$  pressure at 100 °C. The conversion data was obtained by monitoring the changes to absorptions at 1730  $\text{cm}^{-1}$  (PCHC) and 1089  $\text{cm}^{-1}$  (PCHO). The turn-over-frequency was obtained from 20-80.0% PA conversion.

#### Section S4: Synthesis and Characterisation of $\text{H}_2\text{L}^3$ and $3_{\text{ZnNa}}$ and Polymerisation kinetics of $3_{\text{ZnNa}}$



**Scheme S 3:** Synthesis of  $\text{H}_2\text{L}^3$  from **A** and NMR assignment numbering for  $\text{H}_2\text{L}^3$

**Synthesis of  $\text{H}_2\text{L}^3$ :** A solution of **A** (71.6 mg, 0.28 mmol, 1 equiv.) in acetonitrile (4 mL) was added to a solution of 4,5-dichlorophenylenediamine (48.9 mg, 0.28 mmol,

1 equiv.) in acetonitrile (4 mL). The mixture was allowed to stand for one week at room temperature during which brown crystals formed, which were isolated by decantation, washed with Et<sub>2</sub>O (1mL) and dried under vacuum to yield H<sub>2</sub>L<sup>3</sup> as a brown crystalline powder (28.5 mg, 35 μmol, 25%).

**<sup>1</sup>H NMR (400 MHz, CDCl<sub>3</sub>)** δ 12.84 (s, 1H, OH), 8.58 (s, 1H, H<sub>4</sub>), 7.31 (s, 1H, H<sub>2</sub>), 7.15 (dd, *J* = 7.8, 1.6 Hz, 1H, H<sub>6</sub>), 7.04 (dd, *J* = 7.9, 1.6 Hz, 1H, H<sub>8</sub>), 6.83 (t, *J* = 7.9 Hz, 1H, H<sub>7</sub>).

**<sup>13</sup>C{<sup>1</sup>H} NMR (126 MHz, CDCl<sub>3</sub>)** δ 164.46 (C<sub>4</sub>), 152.22 (C<sub>10</sub>), 144.58 (C<sub>9</sub>), 142.24 (C<sub>3</sub>), 131.06 (C<sub>1</sub>), 127.31 (C<sub>2</sub>), 122.44 (C<sub>8</sub>), 120.52 (C<sub>6</sub>), 120.15 (C<sub>5</sub>), 118.59 (C<sub>7</sub>).

**Elemental Analysis** (H<sub>2</sub>L<sup>3</sup> · H<sub>2</sub>O, C<sub>40</sub>H<sub>26</sub>Cl<sub>4</sub>N<sub>4</sub>O<sub>7</sub>) calculated C 58.8% H 3.2% N 6.9% found C 58.9% H 3.0% N 7.2%

**HRESI-MS** *m/z* = calculated [M + H]<sup>+</sup> 821.0336; found 821.0322.

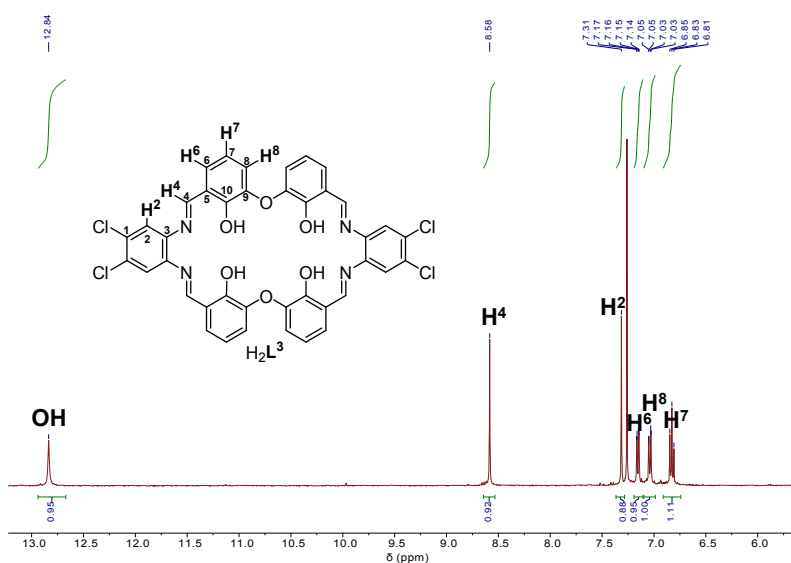


**Figure S 13:** <sup>1</sup>H NMR spectrum (500 MHz, CDCl<sub>3</sub>, 25°C) of H<sub>2</sub>L<sup>3</sup>.

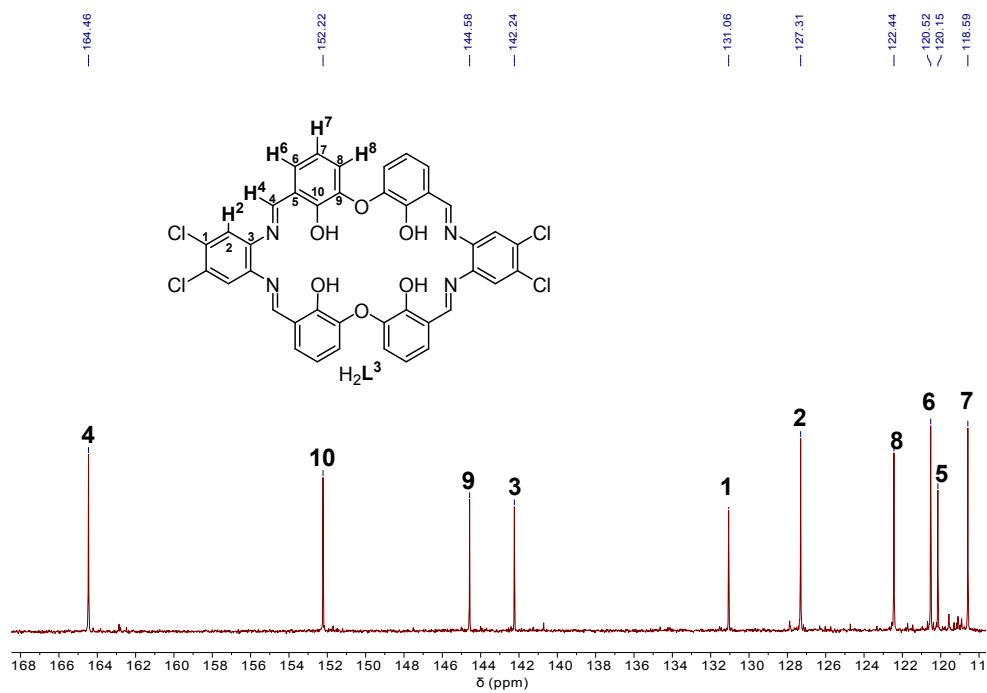


**Figure S 14:**  $^{13}C\{^1H\}$  NMR spectrum (126 MHz,  $CDCl_3$ , 25°C) of  $H_2L^3$ .

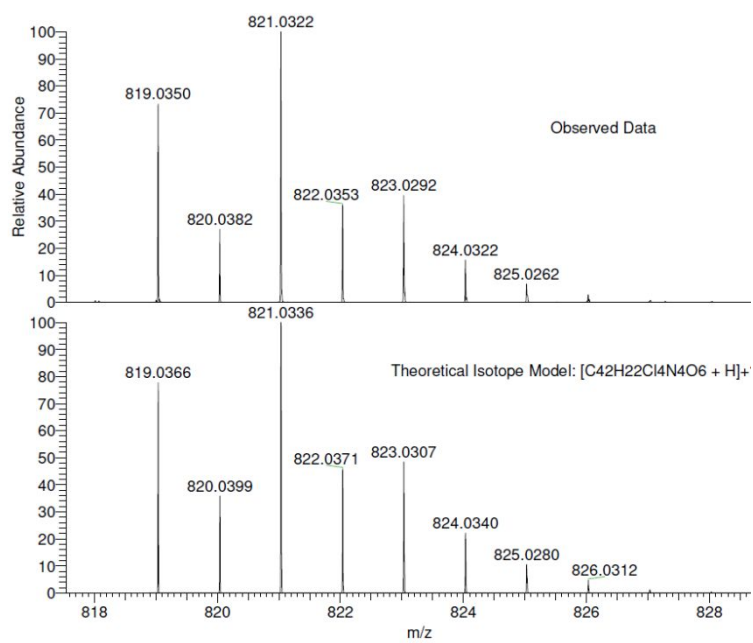
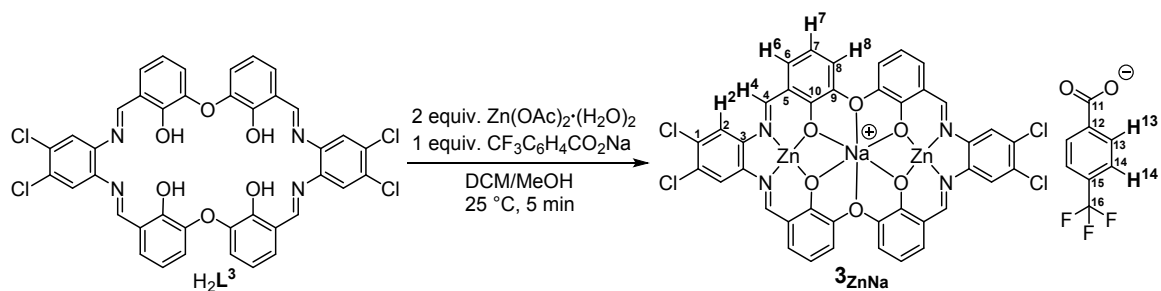


**Figure S 15:** Positive mode high-resolution ESI mass spectrum of  $H_2L^3$ .



**Scheme S 4:** Synthesis of  $3_{\text{ZnNa}}$  from  $\text{H}_2\text{L}^3$  and NMR assignment numbering for  $3_{\text{ZnNa}}$ .

**Synthesis of  $3_{\text{ZnNa}}$ :** A solution of  $\text{Zn}(\text{OAc})_2 \cdot (\text{H}_2\text{O})_2$  (33.3 mg, 151  $\mu\text{mol}$ , 2 equiv.) and  $\text{CF}_3\text{C}_6\text{F}_4\text{CO}_2\text{Na}$  (17.2 mg, 75  $\mu\text{mol}$ , 1 equiv.) in MeOH (5 mL) was added to a solution of  $\text{H}_2\text{L}^3$  (60.0 mg, 75  $\mu\text{mol}$ , 1 equiv.) in 5 mL DCM (5 mL). The resulting solution was stirred for 5 min. Afterwards all volatiles were removed *in vacuo* yielding a semi-solid which was washed with  $\text{Et}_2\text{O}$  (100 mL). To remove the acetic acid by-product fully, the crude product was suspended in toluene (20 mL) which was afterwards removed *in vacuo*. This process was repeated, yielding  $3_{\text{ZnNa}} \cdot 5\text{H}_2\text{O}$  as a red powder (87.5 mg, 71  $\mu\text{mol}$ , 95%).

**$^1\text{H}$  NMR (500 MHz,  $\text{d}_6$ -DMSO)**  $\delta$  8.89 (s, 1H, H4), 8.12 (s, 1H, H2), 7.96 (s, 0.5H, H13), 7.65 (s, 0.5H, H14), 7.21 (d,  $J = 8.0$  Hz, 1H, H6), 7.17 (d,  $J = 7.9$  Hz, 1H, H8), 6.54 (t,  $J = 7.8$  Hz, 1H, H7).

**$^{13}\text{C}\{^1\text{H}\}$  NMR (126 MHz,  $\text{d}_6$ -DMSO)**  $\delta$  167.88 (C11), 165.93 (C4), 163.40 (C3), 148.89 (C9), 140.85 (C10), 135.42 (C12), 131.91 (C6), 130.33 (C1), 129.85 (C13), 128.69, 125.01 (C14), 124.27 (m, C15, C5), 121.82 (C8), 119.71 (C2), 112.65 (C7).

**$^{19}\text{F}\{^1\text{H}\}$  NMR (470 MHz,  $\text{d}_6$ -DMSO)**  $\delta$  -61.01.

**Elemental Analysis ( $3_{\text{ZnNa}} \cdot 5\text{H}_2\text{O}$ ,  $\text{C}_{48}\text{H}_{34}\text{Cl}_4\text{F}_3\text{N}_4 \text{NaO}_{13}\text{Zn}_2$ )** calculated C 47.0% H 2.8% N 4.4% found C 47.0% H 2.5% N 4.4%

**HRESI-MS  $m/z$**  = calculated  $[\text{M} - \text{CF}_3\text{C}_6\text{F}_4\text{CO}_2\text{Na}]^+$  946.8560. Found 946.8564

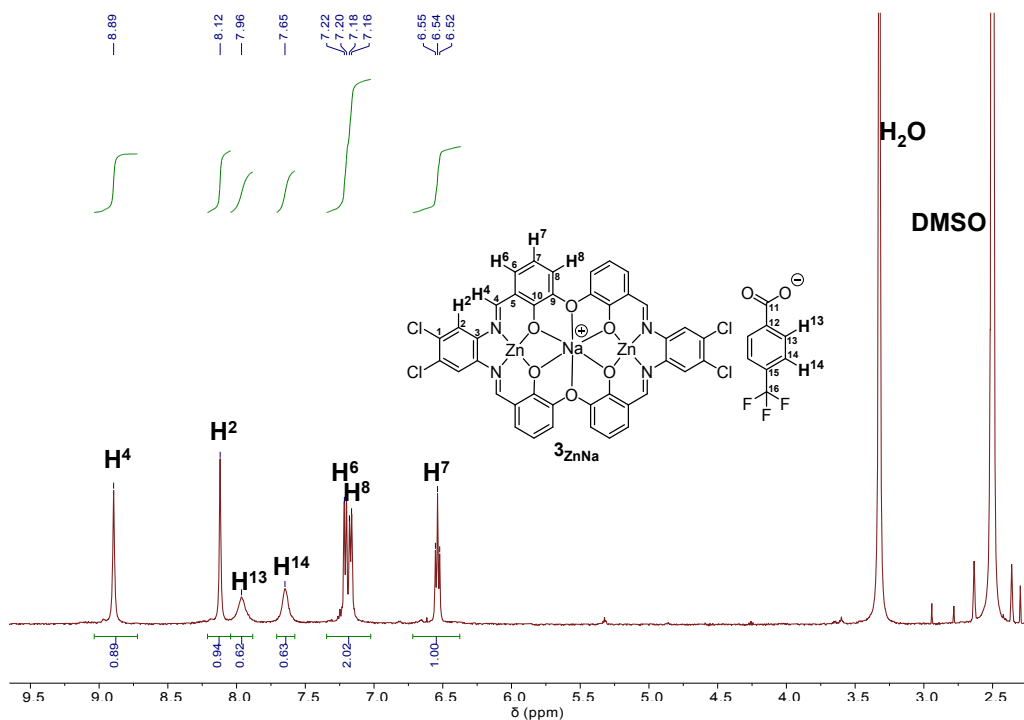


**Figure S 16:  $^1\text{H}$  NMR spectrum (500 MHz,  $d_6$ -DMSO, 25°C) of  $3\text{ZnNa}$ .**

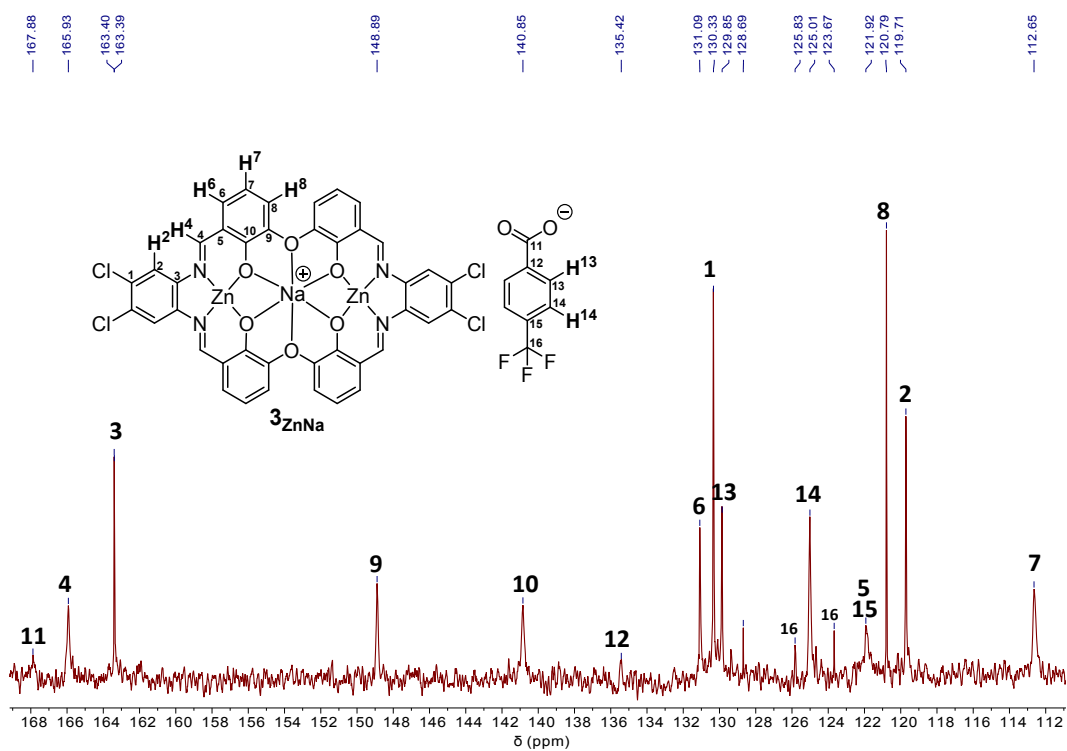


**Figure S 17:  $^{13}\text{C}\{^1\text{H}\}$  NMR spectrum (126 MHz,  $d_6$ -DMSO, 25°C) of  $3\text{ZnNa}$ .**

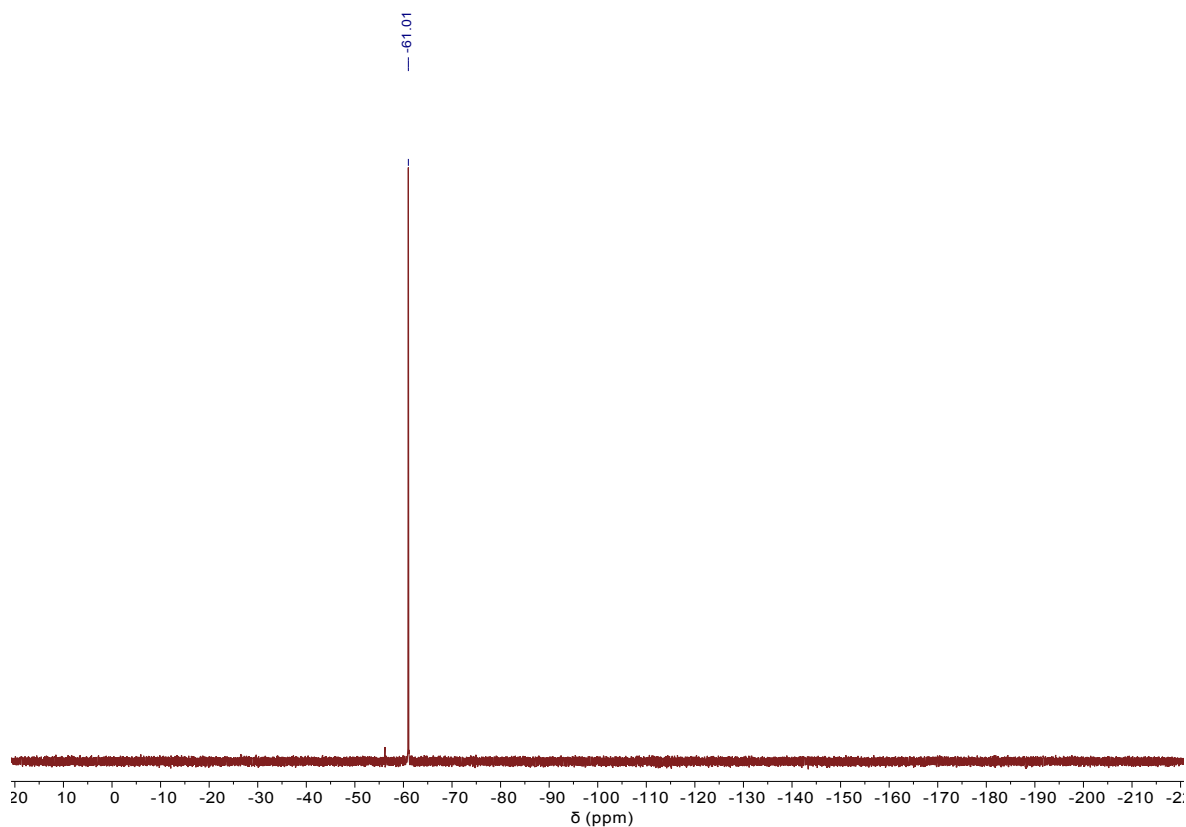


Figure S 18:  $^{19}\text{F}\{^1\text{H}\}$  NMR (470 MHz,  $d_6$ -DMSO,  $25^\circ\text{C}$ ) of  $3_{\text{ZnNa}}^+$ .

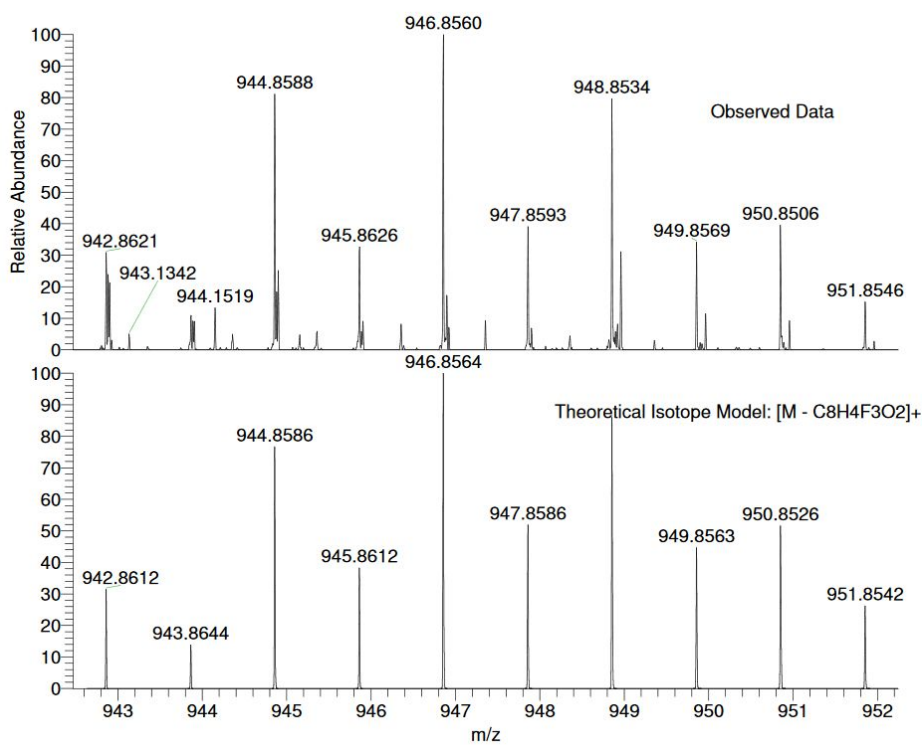
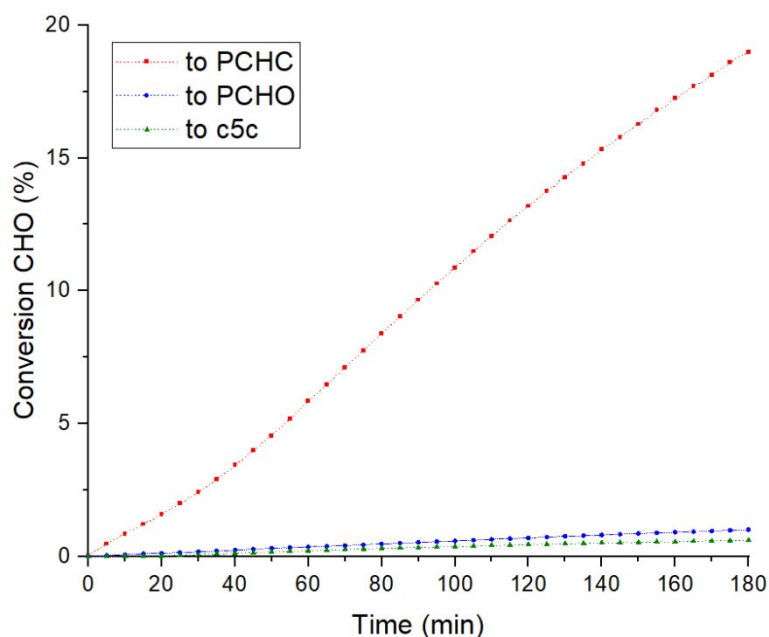
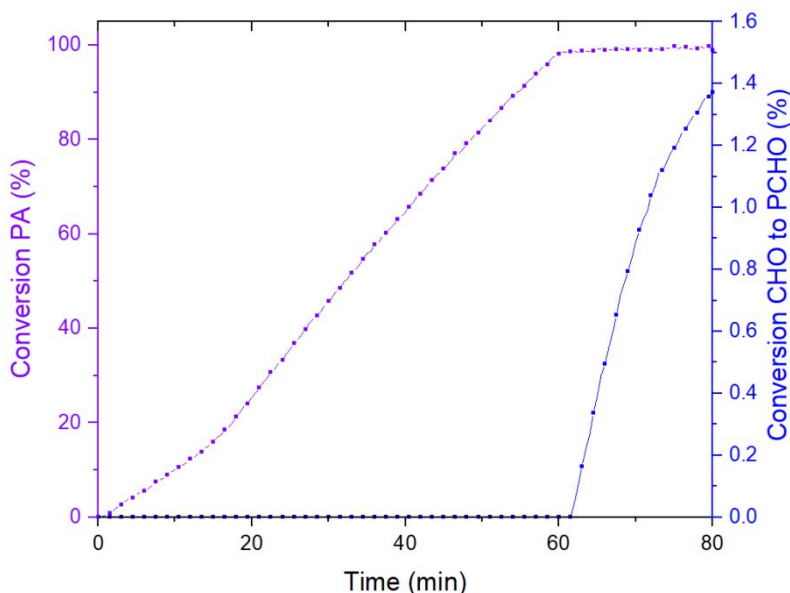


Figure S 19: Positive mode high-resolution ESI mass spectrum of  $3_{\text{ZnNa}}^+$ .



**Figure S 20:** Plot showing conversion of CHO to polymer (PCHC and PCHO) and c5c vs. time (

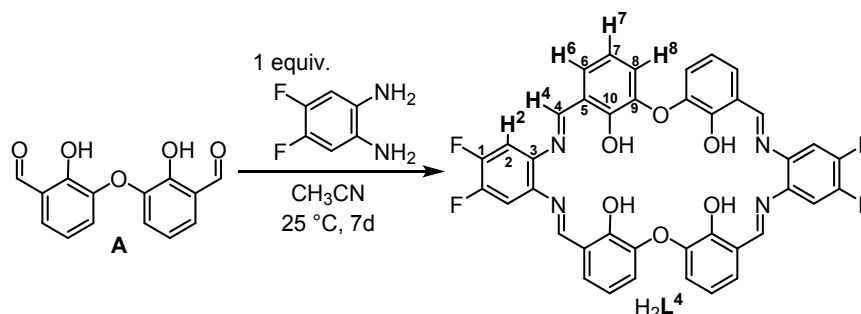
**Table S 1**, run #3). Data are obtained using *in situ* ATR-IR spectroscopic monitoring of polymerizations conducted using 1 equiv.  $\mathbf{3}_{ZnNa}$ , 20 equiv. cyclohexane diol (CHD), 4000 equiv. cyclohexene oxide (CHO) and 1 bar carbon dioxide pressure at 100 °C. The conversion data was obtained by monitoring the changes to absorptions at 1744  $\text{cm}^{-1}$  (PCHC), 1089  $\text{cm}^{-1}$  (PCHO) and 1785  $\text{cm}^{-1}$  (c5c). The turn-over-frequency (TOF) was obtained from 5-15.0% conversion to PCHC.



**Figure S 21:** Plot showing conversion of PA and CHO to polymer (PCHPE and PCHO respectively) vs. time (**Table S 2**, run #3). Data are obtained using *in situ* ATR-IR spectroscopic monitoring of polymerizations conducted using 1 equiv.  $\mathbf{Zn}_2\mathbf{Na}$ , 20 equiv. cyclohexane diol (CHD), 200 equiv. PA, 4000 equiv. cyclohexene oxide (CHO)

and 1 bar N<sub>2</sub> pressure at 100 °C. The conversion data was obtained by monitoring the changes to absorptions at 1730 cm<sup>-1</sup> (PCHC) and 1089 cm<sup>-1</sup> (PCHO). The turn-over-frequency was obtained from 20-80.0% PA conversion.

### Section S5: Synthesis and Characterisation of H<sub>2</sub>L<sup>4</sup> and 4<sub>ZnNa</sub> and Polymerisation kinetics of 4<sub>ZnNa</sub>



**Scheme S 5:** Synthesis of H<sub>2</sub>L<sup>4</sup> and NMR assignment numbering for H<sub>2</sub>L<sup>4</sup>.

**Synthesis of H<sub>2</sub>L<sup>2</sup>:** A solution of **A** (71.6 mg, 0.28 mmol, 1 equiv.) in acetonitrile (4 mL) was added to a solution of 4,5-dimethyl-phenylenediamine (39.8 mg, 0.28 mmol, 1 equiv.) in acetonitrile (4 mL). The mixture was allowed to stand for one week at room temperature during which brown crystals formed, which were isolated by decantation, washed with Et<sub>2</sub>O (1mL) and dried under vacuum to yield H<sub>2</sub>L<sup>4</sup> H<sub>2</sub>O as a brown crystalline powder (29.4 mg, 39 μmol, 28%).

**<sup>1</sup>H NMR (500 MHz, CDCl<sub>3</sub>)** δ 8.80 (s, 1H, H4), 7.44 (t, *J* = 9.5 Hz, 1H, H2), 7.28 (dd, *J* = 7.7, 1.6 Hz, 1H, H6), 6.95 (dd, *J* = 8.0, 1.6 Hz, 1H, H8), 6.82 (t, *J* = 7.9 Hz, 1H, H7).

**<sup>13</sup>C NMR (126 MHz, CDCl<sub>3</sub>)** δ 164.70 (d, *J* = 9.5 Hz, C4), 151.57 (C10), 148.76 (dd, *J* = 251.1, 15.5 Hz, C1), 143.69 (C9), 138.51 (t, *J* = 4.5 Hz, C3), 127.31 (C6), 121.70 (C8), 119.88 (C5), 118.23 (C7), 107.93 (C2).

**Elemental Analysis** (4<sub>ZnNa</sub> H<sub>2</sub>O, C<sub>40</sub>H<sub>26</sub>F<sub>4</sub>N<sub>4</sub>O<sub>7</sub>) calculated C 64.0% H 3.5% N 7.5%  
found C 64.0% H 3.4% N 7.3%

**ESI-MS m/z** = calculated [M + H]<sup>+</sup> 732.2; found 732.0; calculated [M + Na]<sup>+</sup> 755.2;  
found 755.0

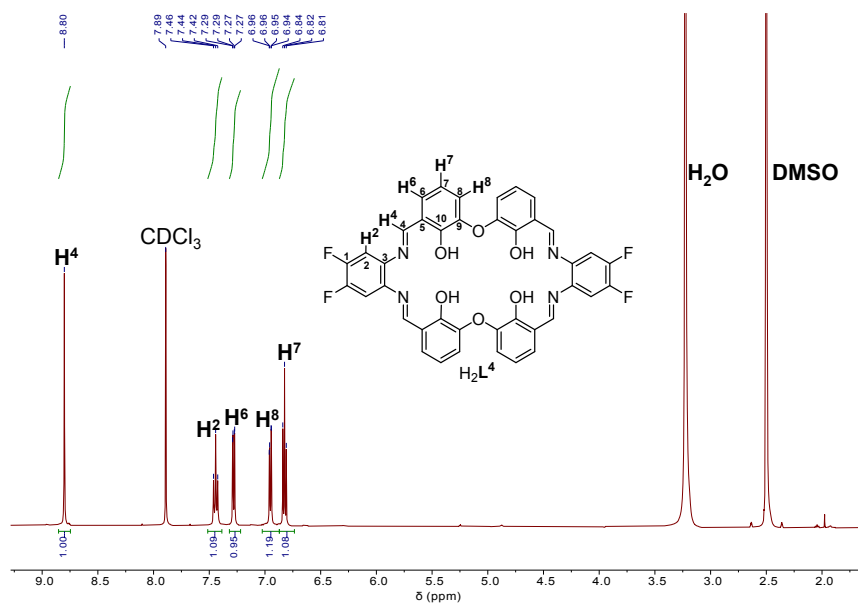


Figure S 22:  $^1\text{H}$  NMR spectrum (500 MHz, 1:1  $\text{CDCl}_3:\text{d}_6\text{-DMSO}$ ,  $25^\circ\text{C}$ ) of  $\text{H}_2\text{L}^4$ .

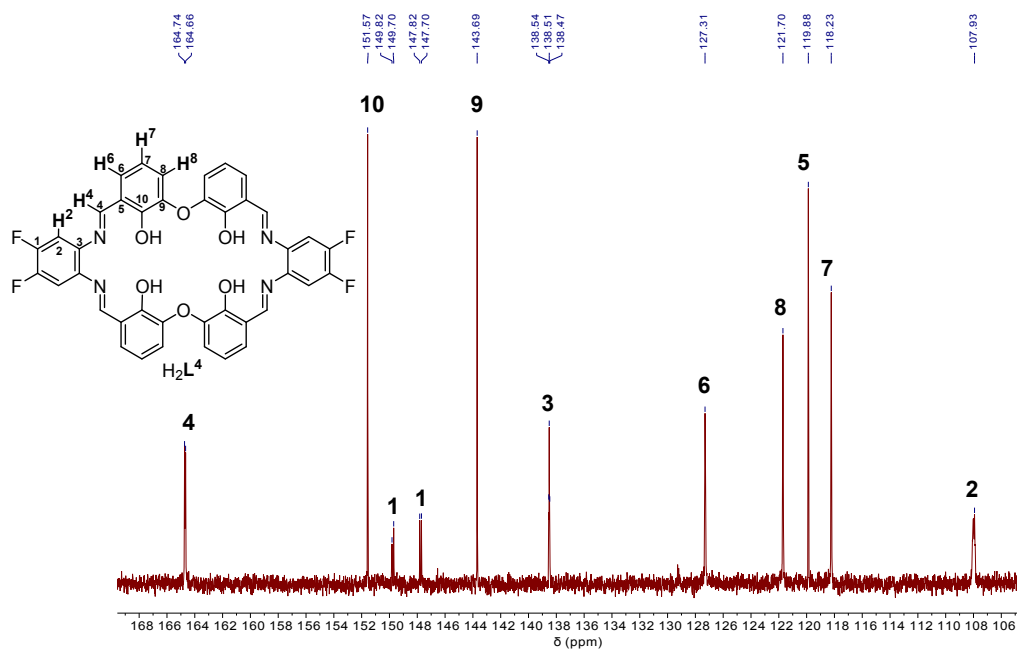


Figure S 23:  $^{13}\text{C}\{^1\text{H}\}$  NMR spectrum (126 MHz, 1:1  $\text{CDCl}_3:\text{d}_6\text{-DMSO}$ ,  $25^\circ\text{C}$ ) of  $\text{H}_2\text{L}^4$ .

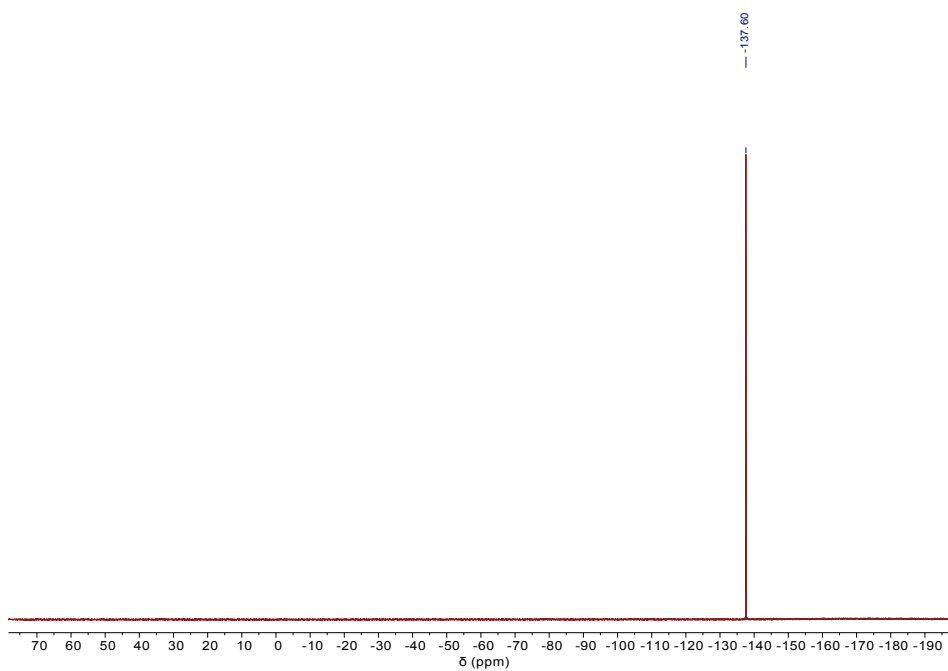


Figure S 24:  $^{19}\text{F}\{^1\text{H}\}$  NMR (470 MHz, 1:1  $\text{CDCl}_3:\text{d}_6\text{-DMSO}$ ,  $25^\circ\text{C}$ ) of  $\text{H}_2\text{L}^4$ .

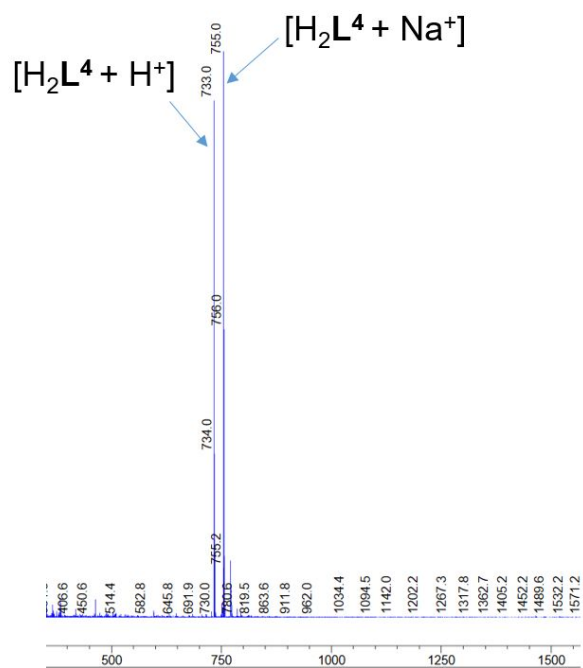
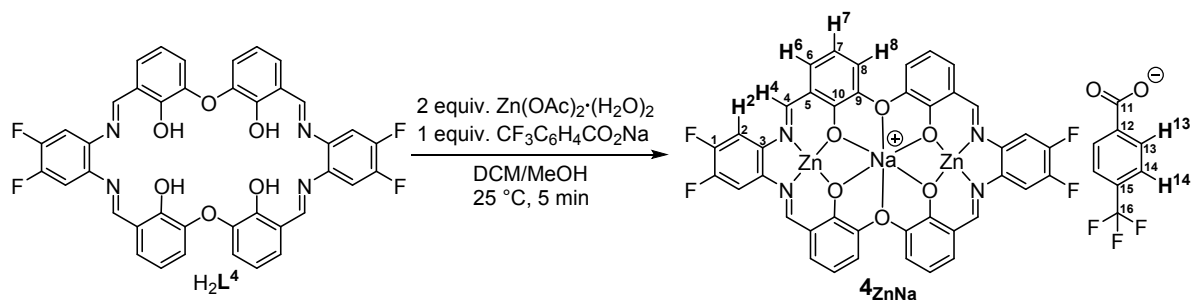


Figure S 25: Positive mode low-resolution ESI mass spectrum of  $4\text{ZnNa}$ .



**Scheme S 6:** Synthesis of  $4_{\text{ZnNa}}$  from  $\text{H}_2\text{L}^4$  and NMR assignment numbering for  $4_{\text{ZnNa}}$ .

**Synthesis of  $4_{\text{ZnNa}}$ :** A solution of  $\text{Zn}(\text{OAc})_2 \cdot (\text{H}_2\text{O})_2$  (33.3 mg, 151  $\mu\text{mol}$ ) and  $\text{CF}_3\text{C}_6\text{F}_4\text{CO}_2\text{Na}$  (17.2 mg, 75  $\mu\text{mol}$ ) in MeOH (5 mL) was added to a solution of  $\text{H}_2\text{L}^4$  (55.0 mg, 75  $\mu\text{mol}$ ) in 5 mL DCM (5 mL). The resulting solution was left unperturbed for 5 min. Afterwards all volatiles were removed, *in vacuo*, yielding a semi-solid which was washed with  $\text{Et}_2\text{O}$  (100 mL). To remove the acetic acid by-product fully, the crude product was suspended in toluene (20 mL) which was afterwards removed under vacuum. This process was repeated, yielding  $4_{\text{ZnNa}} \cdot 2\text{H}_2\text{O}$  as a orange powder (78.6 mg, 71  $\mu\text{mol}$ , 95%).

**$^1\text{H}$  NMR (500 MHz,  $\text{d}_6$ -DMSO)**  $\delta$  8.80 (s, 1H, H4), 7.90-8.01 (m, 2H, H13, H2), 7.59 (d,  $J = 8.0$  Hz, 1H, H14), 7.17 (d,  $J = 8.0$  Hz, 2H, H6, H8), 6.71 – 6.41 (m, 1H, H7).

**$^{19}\text{F}$  NMR (377 MHz,  $\text{d}_6$ -DMSO)**  $\delta$  -60.90 ( $\text{CF}_3$ ), -138.69 (ArF).

No  $^{13}\text{C}$  NMR could be obtained due to the low solubility of  $4_{\text{ZnNa}}$  in all common organic solvents.

**Elemental Analysis ( $4_{\text{ZnNa}} \cdot 2\text{H}_2\text{O}$ ,  $\text{C}_{48}\text{H}_{48}\text{F}_7\text{N}_4\text{NaO}_{10}\text{Zn}_2$ )** calculated C 52.1% H 2.6% N 5.1% found C 51.7% H 2.7% N 5.1%

**HRESI-MS  $m/z$**  = calculated  $[\text{M} - \text{CF}_3\text{C}_6\text{F}_4\text{CO}_2\text{Na}]^+$  880.9763; found 880.9768.

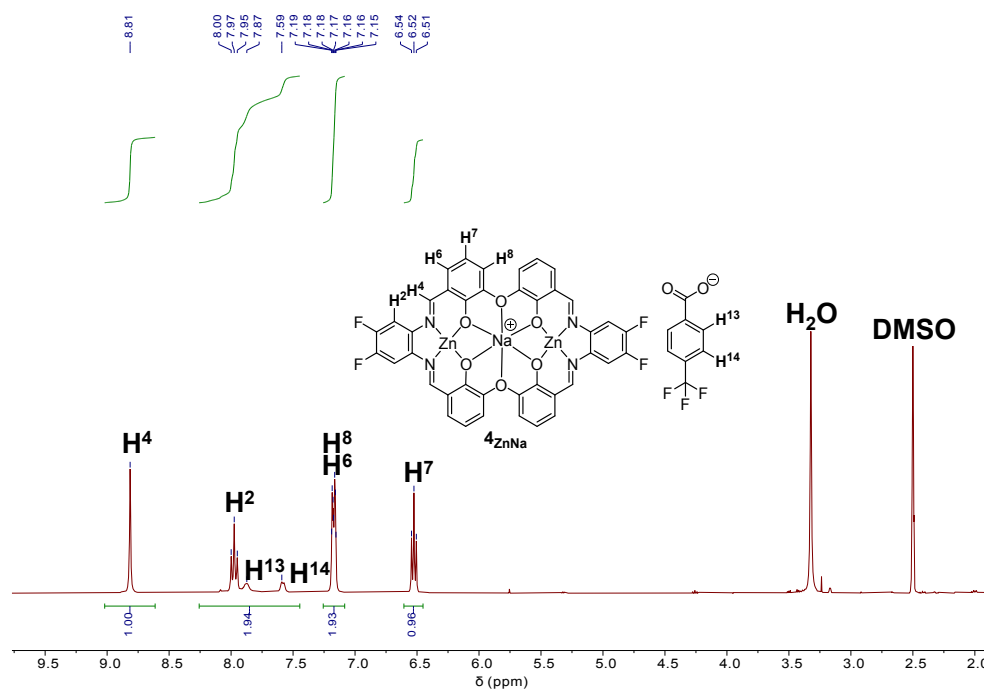


Figure S 26:  $^1H$  NMR spectrum (500 MHz,  $d_6$ -DMSO, 25°C) of  $4ZnNa$ .

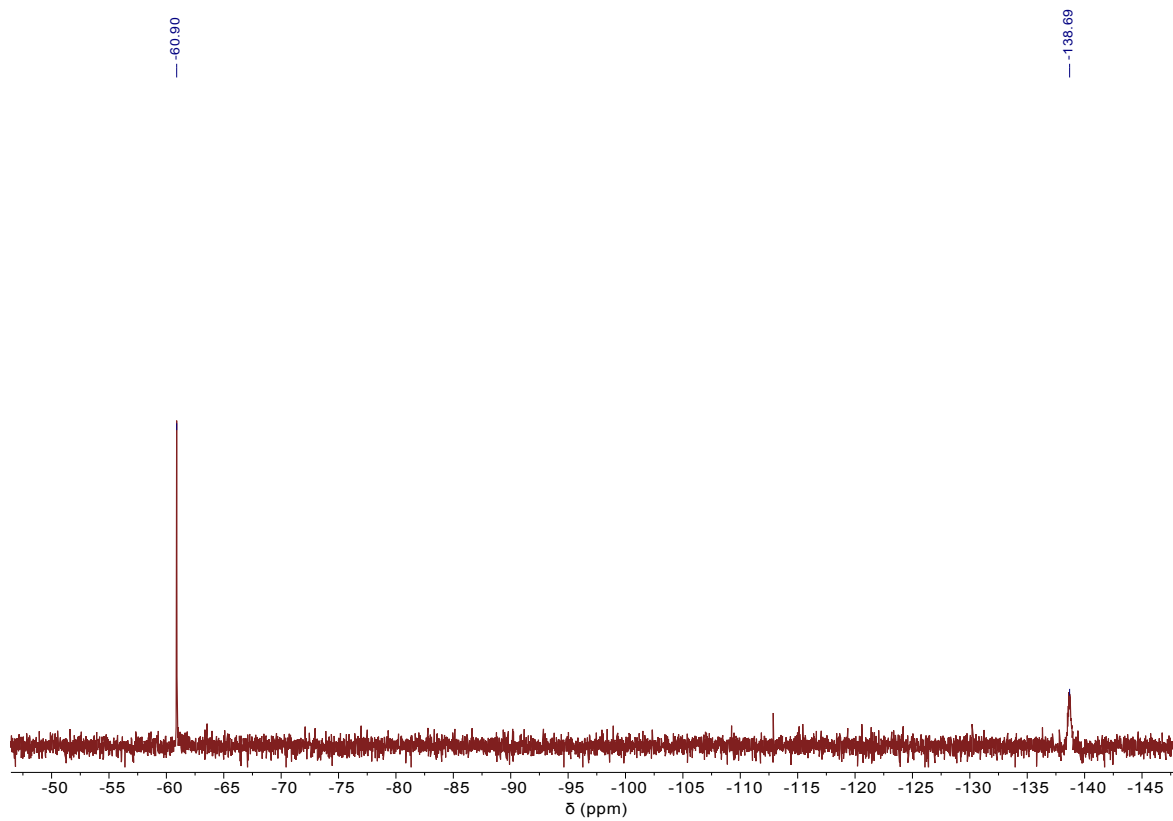
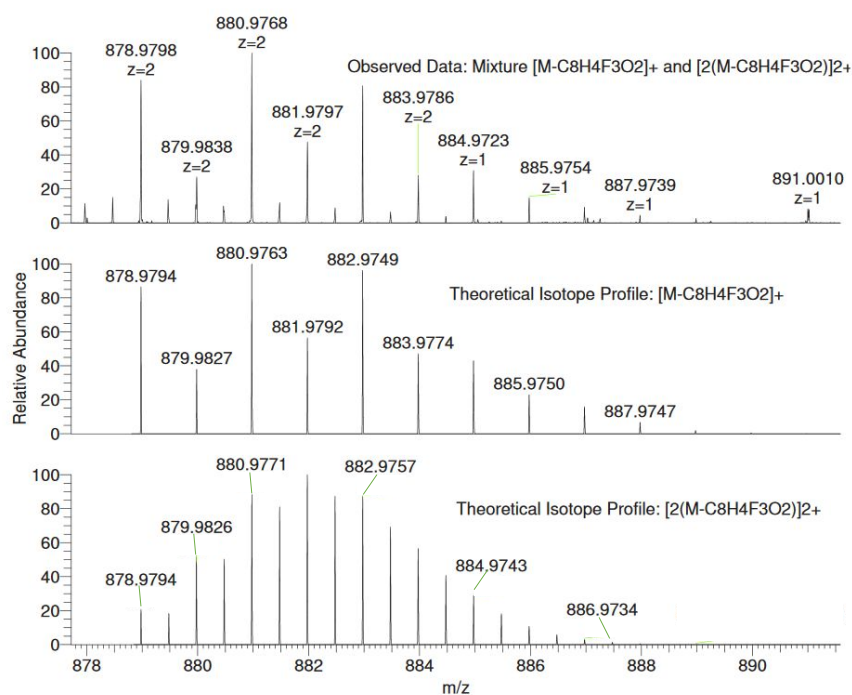
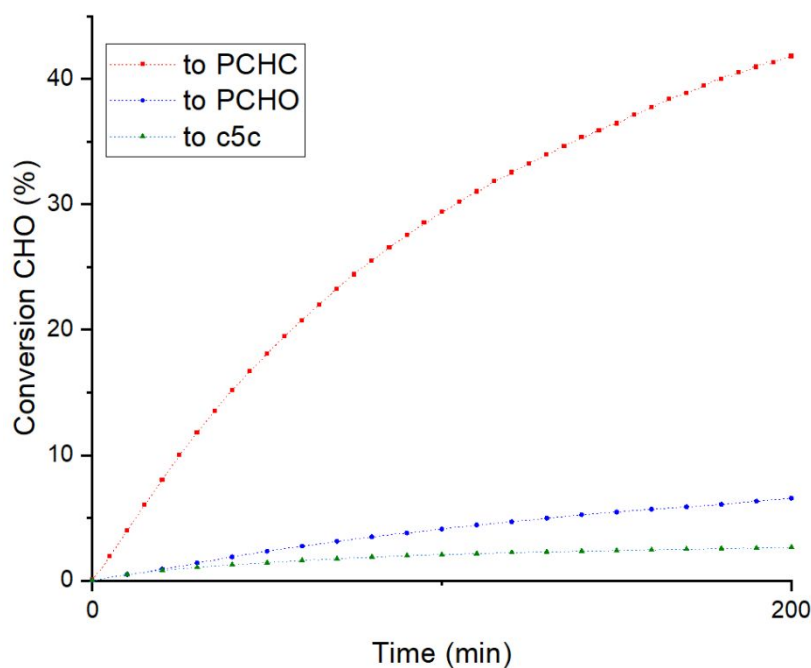


Figure S 27:  $^{19}F$   $\{^1H\}$  NMR (377 MHz,  $d_6$ -DMSO, 25°C) of  $4ZnNa$ .



**Figure S 28:** Positive mode high-resolution ESI mass spectrum of  $4\text{ZnNa}^+$ .



**Figure S 29:** Plot showing conversion of CHO to polymer (PCHC and PCHO) and c5c vs. time (

**Table S 1**, run #4). Data are obtained using *in situ* ATR-IR spectroscopic monitoring of polymerizations conducted using 1 equiv.  $4\text{ZnNa}^+$ , 20 equiv. cyclohexane diol (CHD), 4000 equiv. cyclohexene oxide (CHO) and 1 bar carbon dioxide pressure at 100 °C. The conversion data was obtained by monitoring the changes to absorptions at 1744

$\text{cm}^{-1}$  (PCHC),  $1089 \text{ cm}^{-1}$  (PCHO) and  $1785 \text{ cm}^{-1}$  (c5c). The turn-over-frequency (TOF) was obtained from 5-15.0% conversion to PCHC.

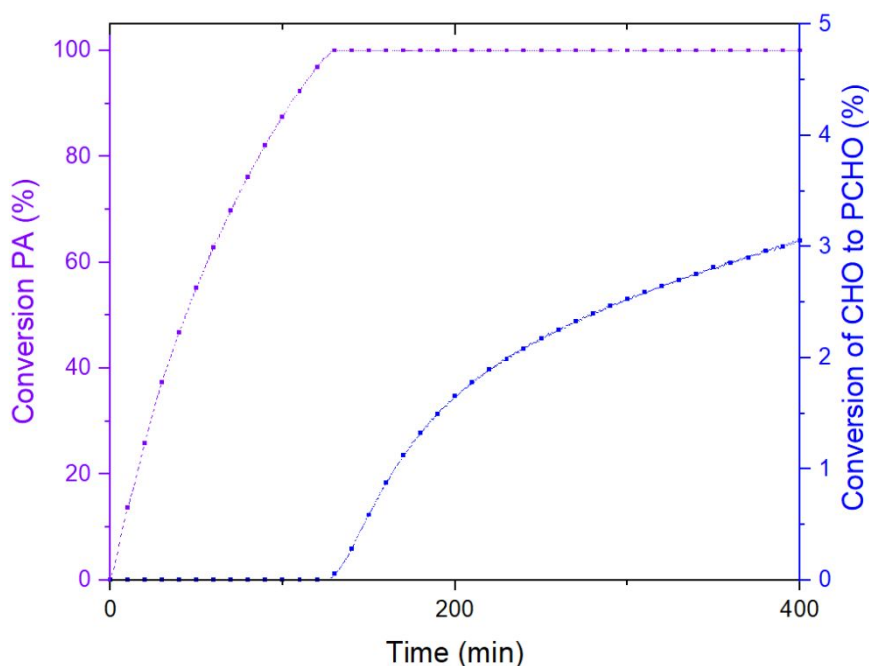
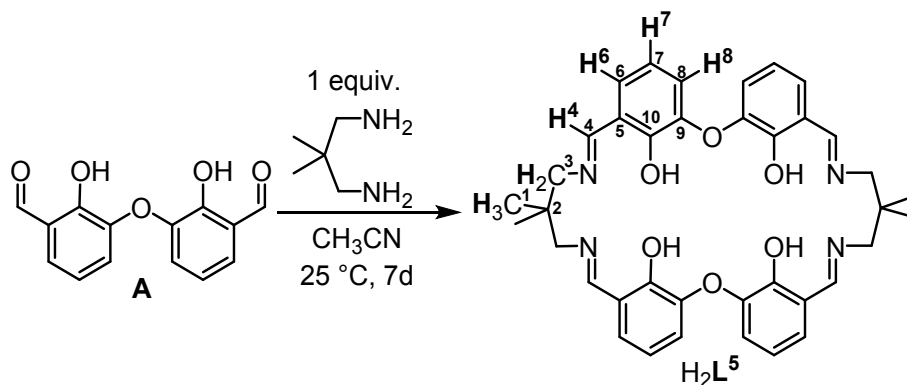


**Figure S 30:** Plot showing conversion of PA and CHO to polymer (PCHPE and PCHO respectively) vs. time (Table S 2, run #4). Data are obtained using *in situ* ATR-IR spectroscopic monitoring of polymerizations conducted using 1 equiv.  $\mathbf{4}_{\text{ZnNa}}$ , 20 equiv. cyclohexane diol (CHD), 200 equiv. PA, 4000 equiv. cyclohexene oxide (CHO) and 1 bar  $\text{N}_2$  pressure at  $100 \text{ }^\circ\text{C}$ . The conversion data was obtained by monitoring the changes to absorptions at  $1730 \text{ cm}^{-1}$  (PCHC) and  $1089 \text{ cm}^{-1}$  (PCHO). The turn-over-frequency was obtained from 0-60.0% PA conversion.

### Section S6: Synthesis and Characterisation of $\text{H}_2\text{L}^5$ and $\mathbf{5}_{\text{ZnNa}}$ and Polymerisation kinetics of $\mathbf{5}_{\text{ZnNa}}$



**Scheme S 7:** Synthesis of  $\text{H}_2\text{L}^5$  and NMR assignment numbering for  $\text{H}_2\text{L}^5$ .

**Synthesis of H<sub>2</sub>L<sup>5</sup>:** A solution of **A** (71.6 mg, 0.28 mmol, 1 equiv.) in acetonitrile (4 mL) was added to a solution of 2,2-dimethyl-1,3-diaminopropylene (28.6 mg, 0.28 mmol, 1 equiv.) in acetonitrile (4 mL). After the mixture was allowed to stand for 24h at room temperature during which a yellow powder precipitated, which was isolated by centrifugation, washed with Et<sub>2</sub>O (1mL) and dried under vacuum to yield H<sub>2</sub>L<sup>5</sup>·H<sub>2</sub>O as a yellow powder (71.0 mg, 0.11 mmol, 77%).

**<sup>1</sup>H NMR (400 MHz, CDCl<sub>3</sub>)** δ 13.94 (s, 1H, OH), 8.36 (s, 1H, H<sub>4</sub>), 7.02 (d, *J* = 7.7 Hz, 1H, H<sub>6</sub>), 6.97 (d, *J* = 7.8 Hz, 1H, H<sub>8</sub>), 6.77 (t, *J* = 7.5 Hz, 1H, H<sub>7</sub>), 3.49 (s, 2H, CH<sub>2</sub>), 1.06 (s, 2H, CH<sub>3</sub>).

**<sup>13</sup>C NMR (126 MHz, CD<sub>2</sub>Cl<sub>2</sub>)** δ 166.29, 153.28, 145.15, 126.53, 121.61, 120.29, 118.32, 68.12, 36.55, 24.44.

**Elemental Analysis** (H<sub>2</sub>L<sub>5</sub>·H<sub>2</sub>O, C<sub>38</sub>H<sub>42</sub>N<sub>4</sub>O<sub>7</sub>) calculated C 68.5% H 6.4% N 8.4%  
found C 68.4% H 6.3% N 8.6%

**HRESI-MS** *m/z* = calculated [M + H]<sup>+</sup> 649.3021, [M + Na]<sup>+</sup> 671.2840. Found [M + H]<sup>+</sup> 649.3018, [M + Na]<sup>+</sup> 671.2937

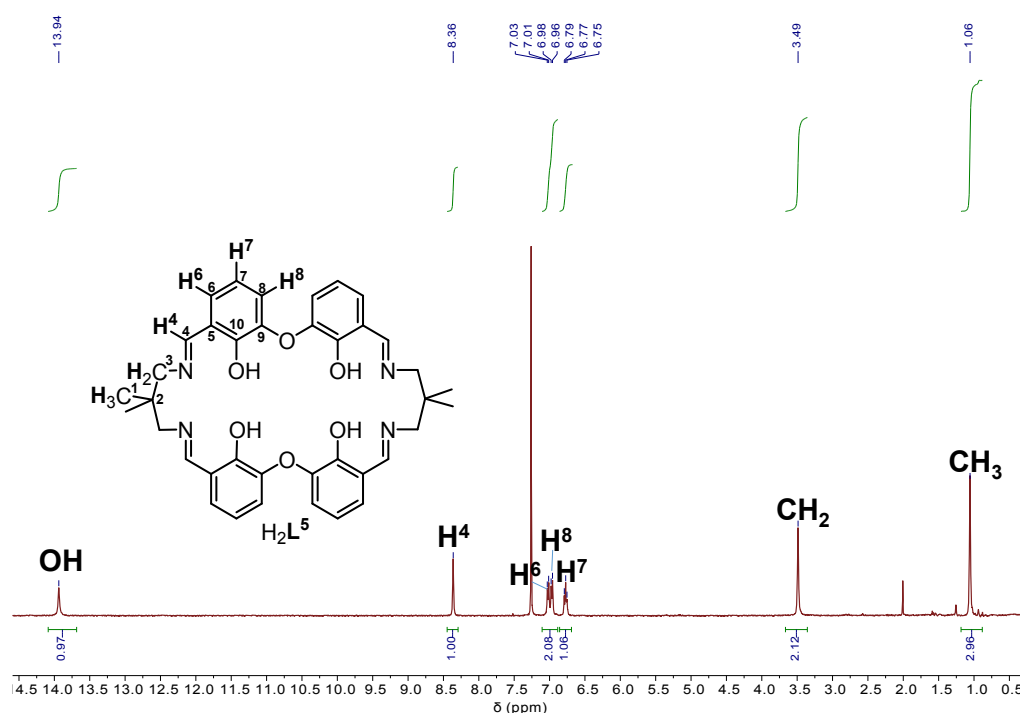


**Figure S 31:** <sup>1</sup>H NMR spectrum (500 MHz, CDCl<sub>3</sub>, 25°C) of H<sub>2</sub>L<sup>5</sup>.

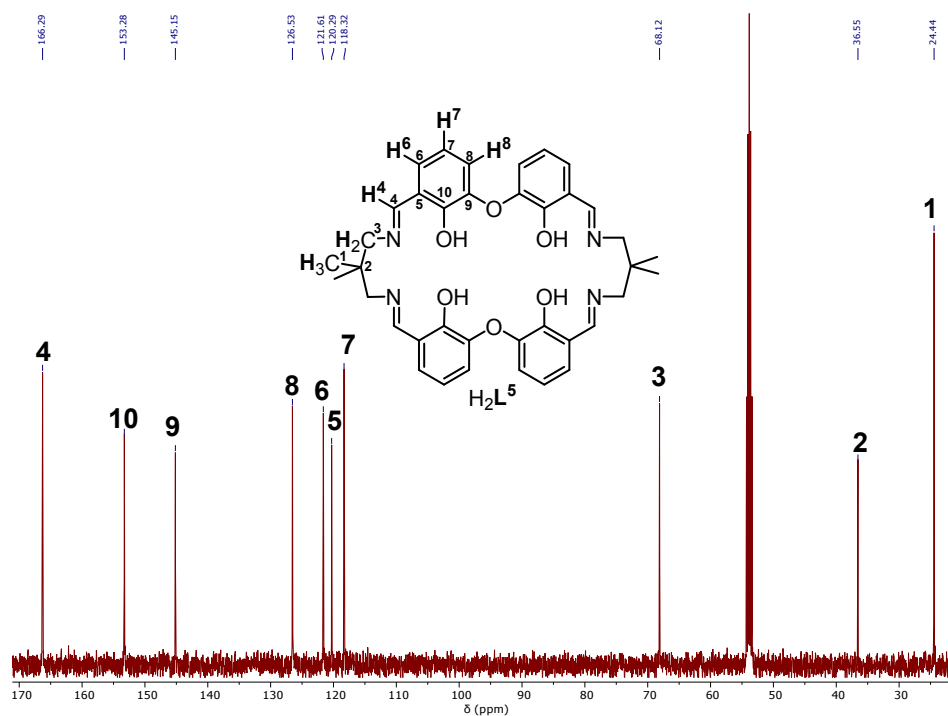


Figure S 32:  $^{13}\text{C}\{^1\text{H}\}$  NMR spectrum (126 MHz,  $\text{d}_6\text{-DMSO}$ ,  $25^\circ\text{C}$ ) of  $\text{H}_2\text{L}^5$ .

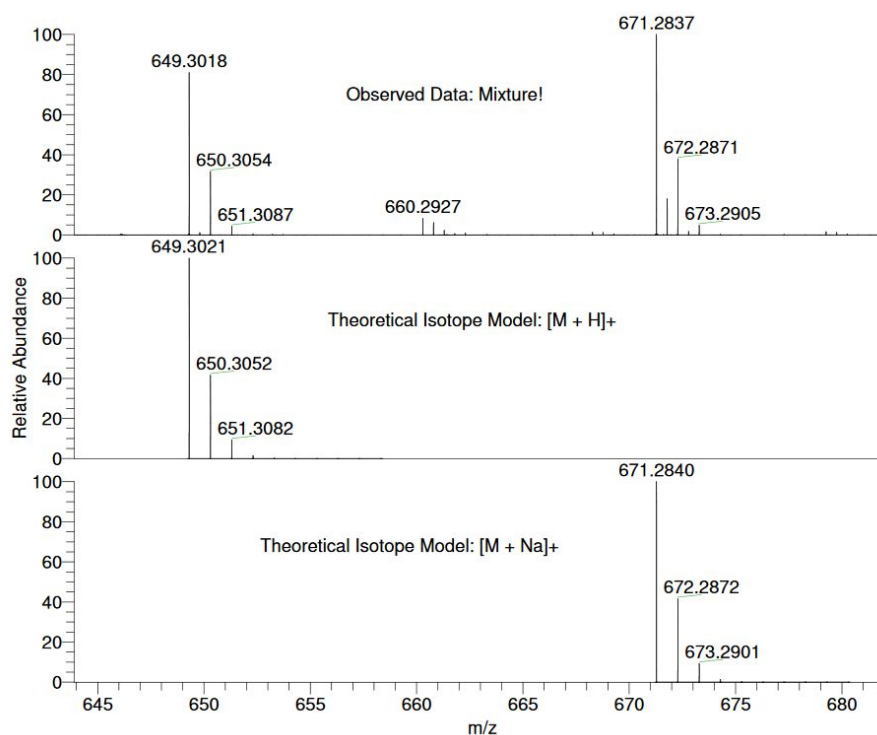
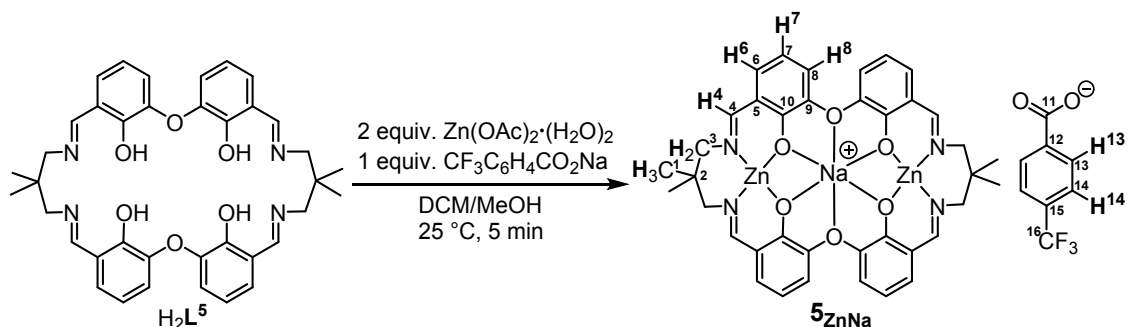


Figure S 33: Positive mode high-resolution ESI mass spectrum of  $\text{H}_2\text{L}^5$ .



**Scheme S 8:** Synthesis of  $5_{\text{ZnNa}}$  and NMR assignment numbering for  $5_{\text{ZnNa}}$ .

**Synthesis of  $5_{\text{ZnNa}}$ :** A solution of  $\text{Zn}(\text{OAc})_2 \cdot (\text{H}_2\text{O})_2$  (33.3 mg, 151  $\mu\text{mol}$ , 2 equiv.) and  $\text{CF}_3\text{C}_6\text{H}_4\text{CO}_2\text{Na}$  (17.2 mg, 75  $\mu\text{mol}$ , 1 equiv.) in MeOH (5 mL) was added to a solution of  $\text{H}_2\text{L}^5$  (55.0 mg, 75  $\mu\text{mol}$ , 1 equiv.) in DCM (5 mL). The resulting solution was left stirred for 5 min. Afterwards all volatiles were removed *in vacuo*, yielding a semi-solid which was washed with  $\text{Et}_2\text{O}$  (100 mL). To remove the acetic acid by-product fully, the crude product was suspended in toluene (20 mL) which was afterwards removed under vacuum. This process was repeated, yielding  $5_{\text{ZnNa}}$  as a yellow powder (74.6 mg, 71  $\mu\text{mol}$ , 95%).

**$^1\text{H}$  NMR (500 MHz,  $\text{d}_4$ -Tetrachloroethane,  $110^\circ\text{C}$ )**  $\delta$  9.34 (s, 1H, H3), 9.23 (d,  $J$  = 7.9 Hz, 1H, H13/H14), 8.78 (d,  $J$  = 7.4 Hz, 1H, H13/H14), 8.41 (s, 1H, H6/H8), 8.18 (s, 1H, H6/H8), 7.77 (s, 1H, H7), 4.95 (s, 2H,  $\text{CH}_2$ ), 2.32 (s, 3H,  $\text{CH}_3$ ).

Due to the fluxional nature of  $5_{\text{ZnNa}}$  no  $^{13}\text{C}$  NMR spectrum could be obtained.

**Elemental Analysis ( $5_{\text{ZnNa}}$   $3.5\text{H}_2\text{O}$ ,  $\text{C}_{46}\text{H}_{47}\text{F}_3\text{N}_4\text{NaO}_{11.5}\text{Zn}_2$ )** calculated C 52.6% H 4.5% N 5.3% found C 53.0% H 4.3% N 4.9%

**$^{19}\text{F}$  NMR (377 MHz,  $\text{d}_4$ -Tetrachloroethane,  $25^\circ\text{C}$ )**  $\delta$  -62.86.

**HRESI-MS  $m/z$**  = calculated  $[\text{M} - \text{CF}_3\text{C}_6\text{H}_4\text{CO}_2\text{Na}]^+$  707.1084; found 707.1022.

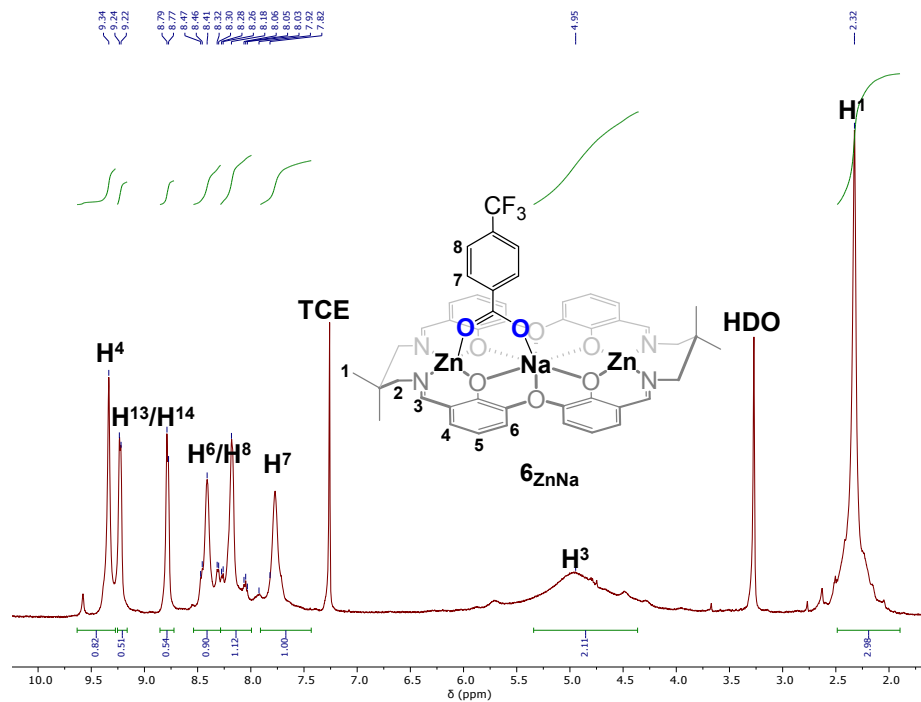


**Figure S 34:**  $^1H$  NMR spectrum (500 MHz,  $d_2$ -TCE, 110°C) of  $5_{ZnNa}$ . Note that this is the temperature limit of the TCE which is why full symmetrisation couldn't be achieved.

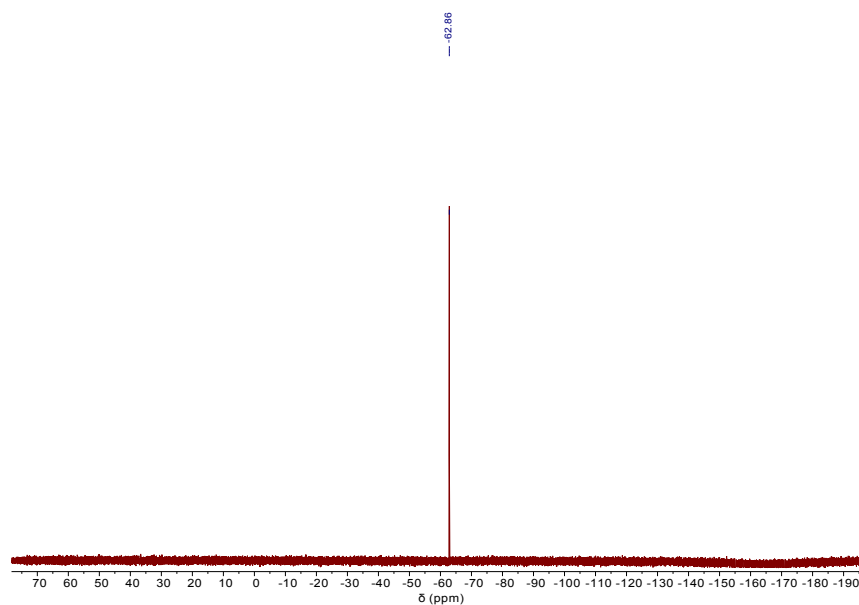


**Figure S 35:**  $^{19}F\{^1H\}$  NMR (377 MHz,  $d_6$ -DMSO, 25°C) of  $5_{ZnNa}$ .

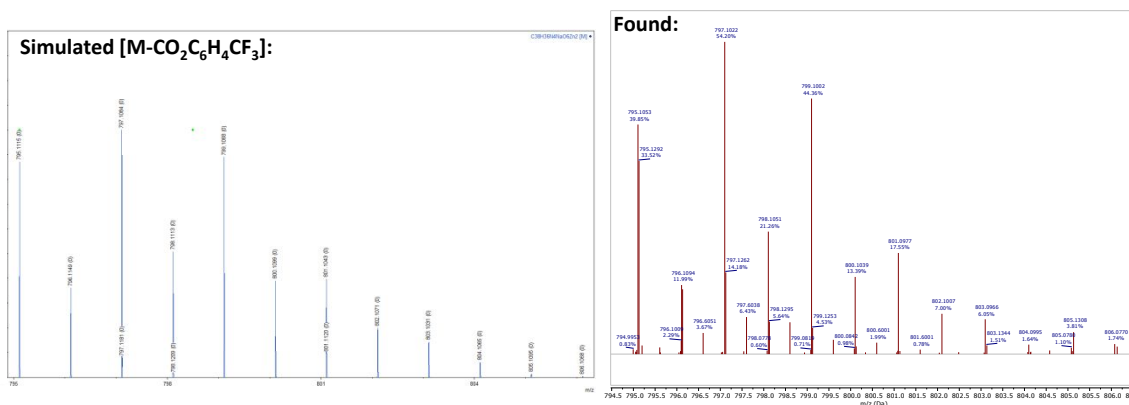


**Figure S 36:** Positive mode high-resolution ESI mass spectrum of **5<sub>ZnNa</sub>**. The data was collected on an Thermo Exactive High-Resolution Orbitrap FTMS.

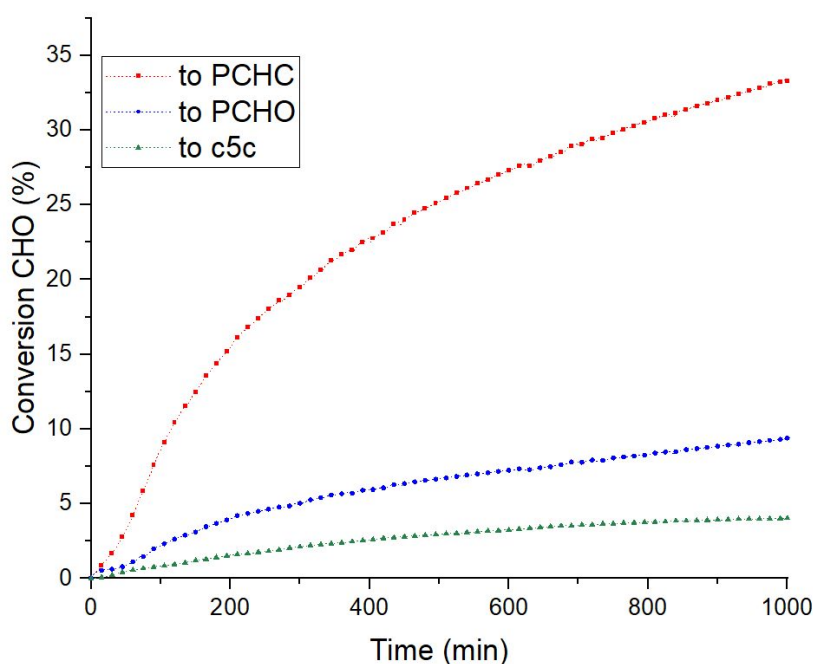


**Figure S 37:** Plot showing conversion of CHO to polymer (PCHC and PCHO) and c5c vs. time (

**Table S 1**, run #5). Data are obtained using *in situ* ATR-IR spectroscopic monitoring of polymerizations conducted using 1 equiv. **5<sub>ZnNa</sub>**, 20 equiv. cyclohexane diol (CHD), 4000 equiv. cyclohexene oxide (CHO) and 1 bar carbon dioxide pressure at 100 °C. The conversion data was obtained by monitoring the changes to absorptions at 1744 cm<sup>-1</sup> (PCHC), 1089 cm<sup>-1</sup> (PCHO) and 1785 cm<sup>-1</sup> (c5c). The turn-over-frequency (TOF) was obtained from 2-12.0% conversion to PCHC.

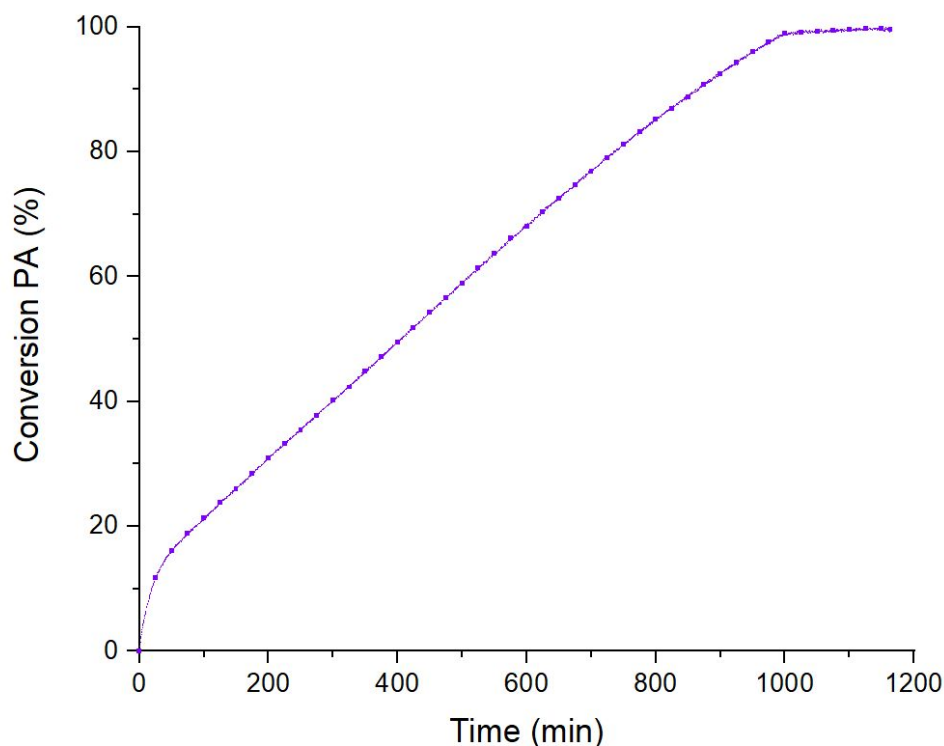
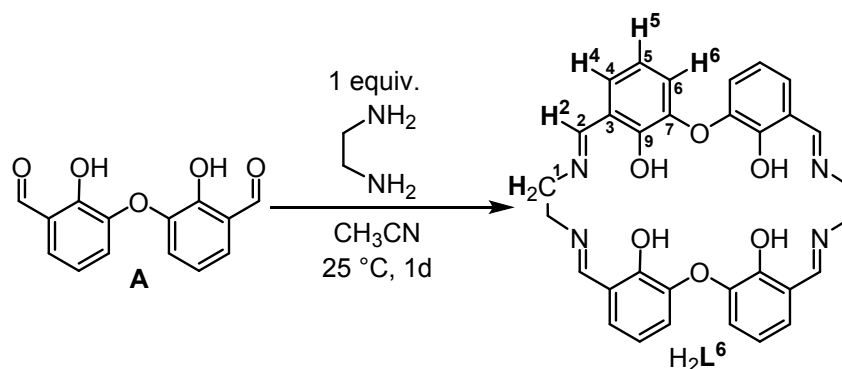


**Figure S 38:** Plot showing conversion of PA and CHO to PCHPE vs. time (**Table S 2**, run #5). Data are obtained using *in situ* ATR-IR spectroscopic monitoring of polymerizations conducted using 1 equiv.  $5_{ZnNa}$ , 20 equiv. cyclohexane diol (CHD), 100 equiv. PA, 4000 equiv. cyclohexene oxide (CHO) and 1 bar  $N_2$  pressure at 100 °C. The conversion data was obtained by monitoring the changes to absorptions at  $1730\text{ cm}^{-1}$  (PCHC). The turn-over-frequency was obtained from 20-80.0% PA conversion.

### Section S7: Synthesis and Characterisation of $H_2L^6$ and $6_{ZnNa}$ and Polymerisation kinetics of $6_{ZnNa}$



**Scheme S 9:** Synthesis of  $H_2L^6$  and NMR assignment numbering for  $H_2L^6$ .

**Synthesis of  $H_2L^6$ :** A solution of **A** (71.6 mg, 0.28 mmol, 1 equiv.) in acetonitrile (4 mL) was added to a solution of 1,2-ethylenediamine (16.8 mg, 0.28 mmol, 1 equiv.) in acetonitrile (4 mL). The mixture was allowed to stand for 24h at room temperature

during which yellow crystals formed, which were isolated by decantation, washed with Et<sub>2</sub>O (1mL) and dried under vacuum to yield H<sub>2</sub>L<sup>6</sup>·0.5H<sub>2</sub>O as a yellow crystalline powder (35.6 mg, 60 μmol, 45%).

**<sup>1</sup>H NMR (500 MHz, d<sub>6</sub>-DMSO)** δ 13.68 (s, 1H, OH), 8.55 (s, 1H, H2), 7.18 (d, *J* = 7.9 Hz, 1H, H4), 6.87 (d, *J* = 7.9 Hz, 1H, H6), 6.75 (t, *J* = 7.9 Hz, 1H, H5), 3.94 (s, 2H, CH<sub>2</sub>).

**<sup>13</sup>C NMR (126 MHz, d<sub>6</sub>-DMSO)** δ 166.27 (C2), 152.88 (C8), 144.35 (C7), 126.88 (C4), 122.22 (C6), 119.87 (C3), 117.45 (C5), 58.24 (C1).

**Elemental Analysis** (H<sub>2</sub>L<sub>6</sub>·0.5H<sub>2</sub>O, C<sub>32</sub>H<sub>29</sub>N<sub>8</sub>NaO<sub>6.5</sub>) calculated C 67.0% H 5.1% N 9.8% found C 67.3% H 4.9% N 9.7%

**HRESI-MS** *m/z* = calculated [M + H]<sup>+</sup> 565.2082, [M + Na]<sup>+</sup> 587.1901. Found [M + H]<sup>+</sup> 565.2071, [M + Na]<sup>+</sup> 587.1887

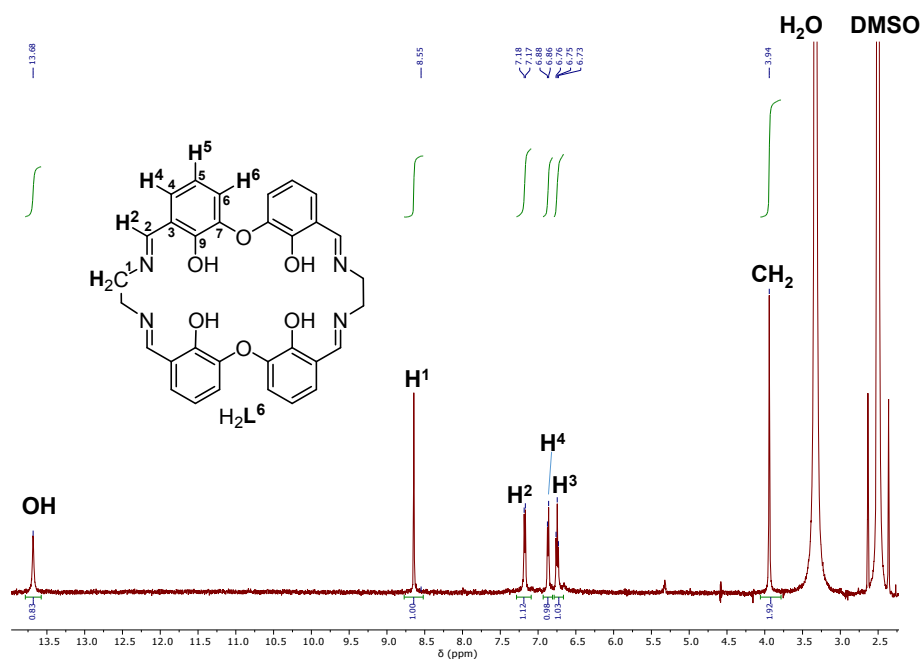


**Figure S 39:** <sup>1</sup>H NMR spectrum (400 MHz, d<sub>6</sub>-DMSO, 25°C) of H<sub>2</sub>L<sup>6</sup>.

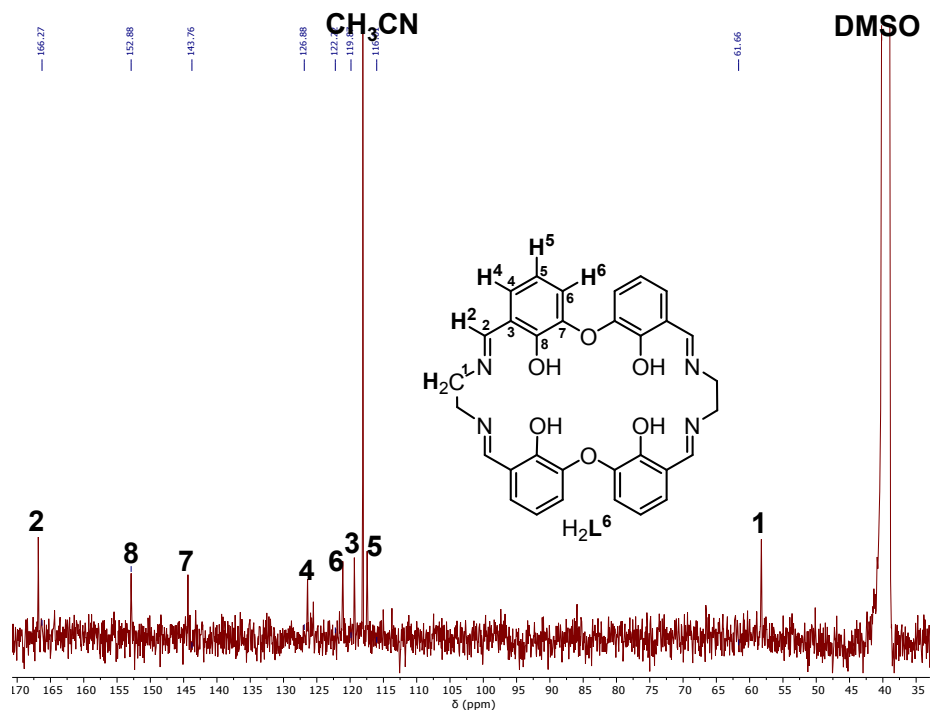


**Figure S 40:**  $^{13}\text{C}\{^1\text{H}\}$  NMR spectrum (126 MHz,  $\text{d}_6\text{-DMSO}$ ,  $25^\circ\text{C}$ ) of  $\text{H}_2\text{L}^6$ .

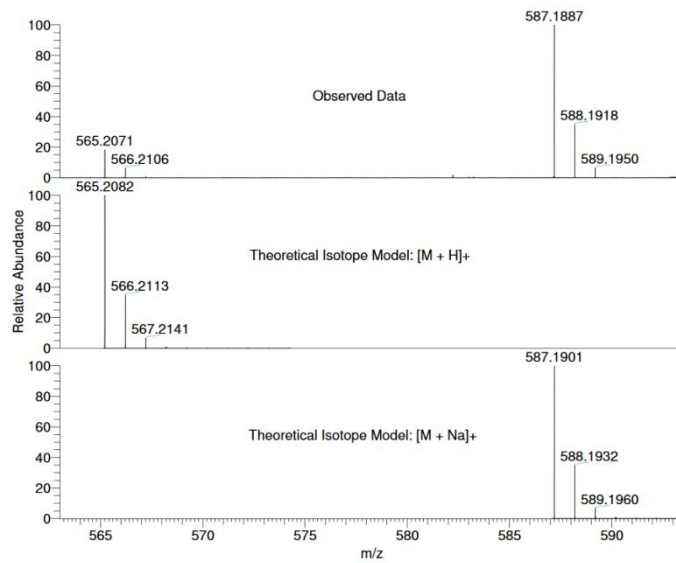
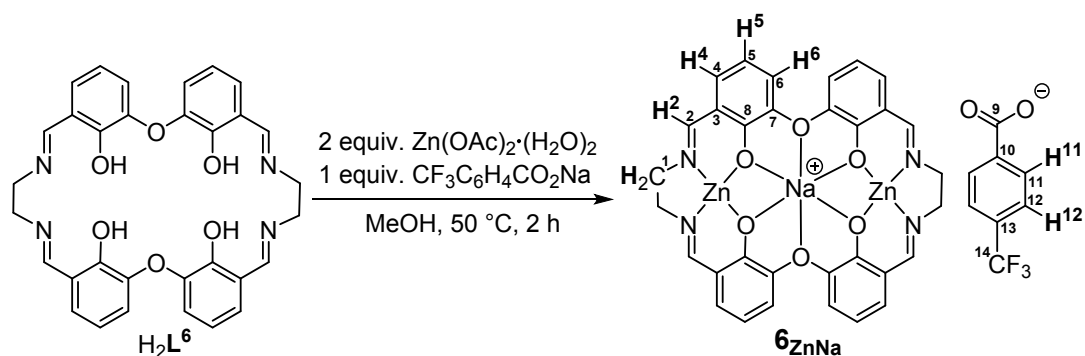


**Figure S 41:** Positive mode high-resolution ESI mass spectrum of  $\text{H}_2\text{L}^6$ .



**Scheme S 10:** Synthesis of  $\mathbf{6}_{\text{ZnNa}}$  and NMR assignment numbering for  $\mathbf{6}_{\text{ZnNa}}$ .

**Synthesis of  $\mathbf{6}_{\text{ZnNa}}$ :** A solution of  $\text{Zn}(\text{OAc})_2 \cdot (\text{H}_2\text{O})_2$  (33.3 mg, 151  $\mu\text{mol}$ , 2 equiv.) and  $\text{CF}_3\text{C}_6\text{H}_4\text{CO}_2\text{Na}$  (17.2 mg, 75  $\mu\text{mol}$ , 1 equiv.) in MeOH (5 mL) was added to solid  $\text{H}_2\text{L}^6$  (42.4 mg, 75  $\mu\text{mol}$ , 1 equiv.). The resulting suspension was stirred at 50°C for 2h during which a clear faint yellow solution formed. Afterwards all volatiles were removed *in vacuo*, yielding a semi-solid which was washed with  $\text{Et}_2\text{O}$  (100 mL). To remove the acetic acid by-product fully, the crude product was suspended in toluene (20 mL) which was afterwards removed under vacuum. This process was repeated, yielding  $\mathbf{6}_{\text{ZnNa}} \cdot 3\text{H}_2\text{O}$  as a faint yellow powder (69.7 mg, 73  $\mu\text{mol}$ , 97%).

**$^1\text{H}$  NMR (500 MHz,  $\text{d}_6\text{-DMSO}$ )**  $\delta$  8.45 (s, 1H, H2), 8.06 (d,  $J = 7.8$  Hz, 1H, H11), 7.68 (d,  $J = 7.9$  Hz, 1H, H12), 7.05 (dd,  $J = 7.7, 1.7$  Hz, 1H, H4), 6.96 (dd,  $J = 8.0, 1.7$  Hz, 1H, H6), 6.41 (t,  $J = 7.8$  Hz, 1H, H5), 3.89 (s, 2H,  $\text{CH}_2$ ).

**$^{13}\text{C}$  NMR (126 MHz,  $\text{d}_6\text{-DMSO}$ )**  $\delta$  168.88 (C9), 168.76 (C2), 162.14 (C8), 148.14 (C7), 141.42 (C13), 130.59 (C10), 130.42 (C11), 129.25 (C4), 125.03 (C12), 124.78 (q,  $J = 272.2$  Hz, C14), 120.94 (C3), 119.21 (C6), 111.29 (C5), 55.01 (C1).

**Elemental Analysis ( $\mathbf{6}_{\text{ZnNa}} \cdot 3\text{H}_2\text{O}$ ,  $\text{C}_{40}\text{H}_{34}\text{F}_3\text{N}_4\text{NaO}_{11}\text{Zn}_2$ )** calculated C 50.2% H 3.6% N 5.9% found C 50.3% H 3.4% N 5.7%

**$^{19}\text{F}$  NMR (377 MHz,  $\text{d}_6\text{-DMSO}$ )**  $\delta$  -60.98.

**HRESI-MS  $m/z$**  = calculated  $[\text{M} - \text{CF}_3\text{C}_6\text{H}_4\text{CO}_2\text{Na}]^+$  711.0171; found 707.0175.

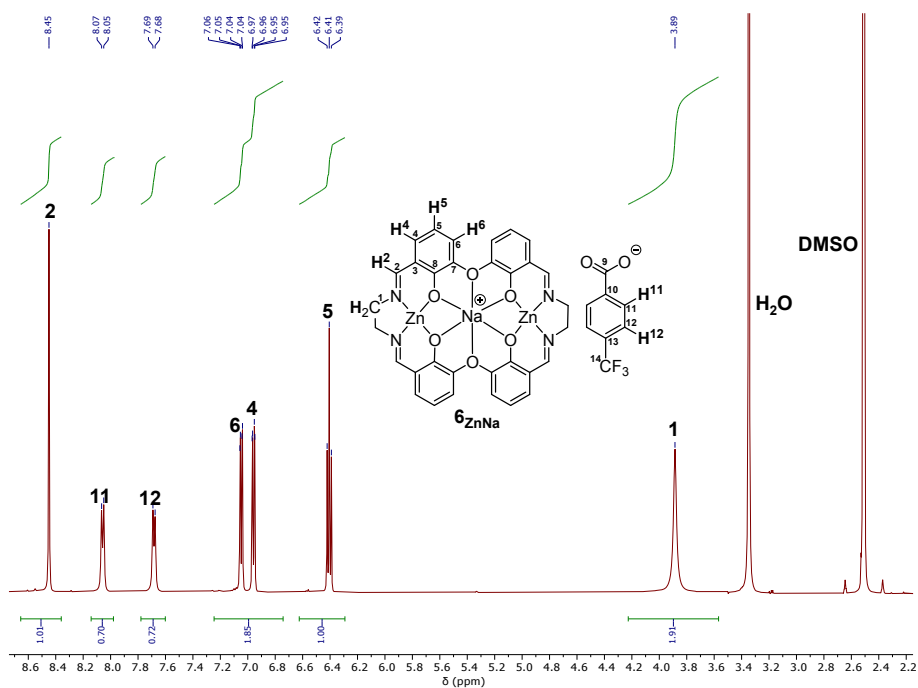


Figure S 42:  $^1\text{H}$  NMR spectrum (400 MHz,  $d_6$ -DMSO, 25°C) of  $6_{\text{ZnNa}}$ .

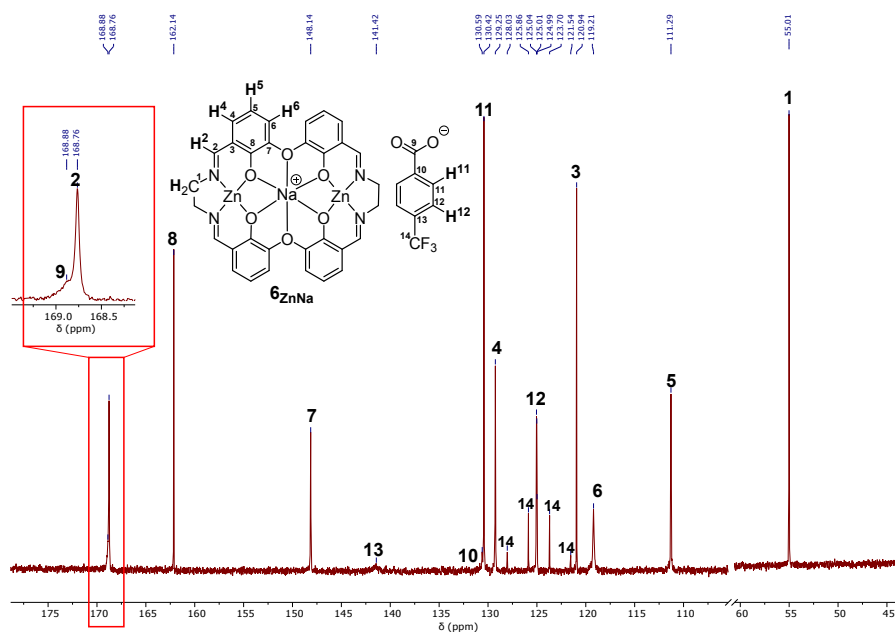


Figure S 43:  $^{13}\text{C}\{^1\text{H}\}$  NMR spectrum (126 MHz,  $d_6$ -DMSO, 25°C) of  $6_{\text{ZnNa}}$ .

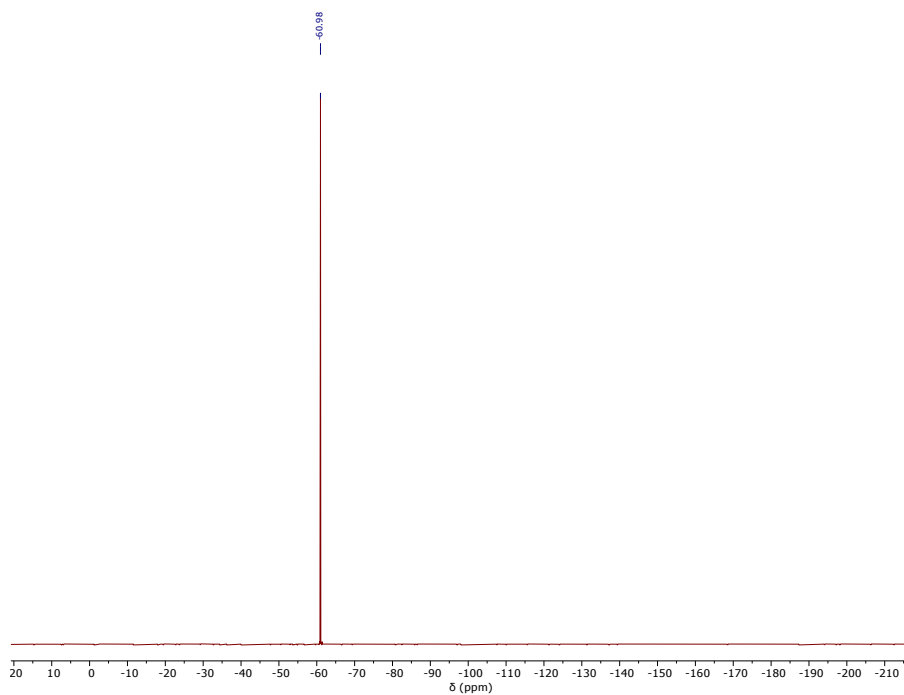


Figure S 44:  $^{19}\text{F}$   $\{^1\text{H}\}$  NMR (377 MHz,  $d_6$ -DMSO,  $25^\circ\text{C}$ ) of  $6_{\text{ZnNa}}$ .

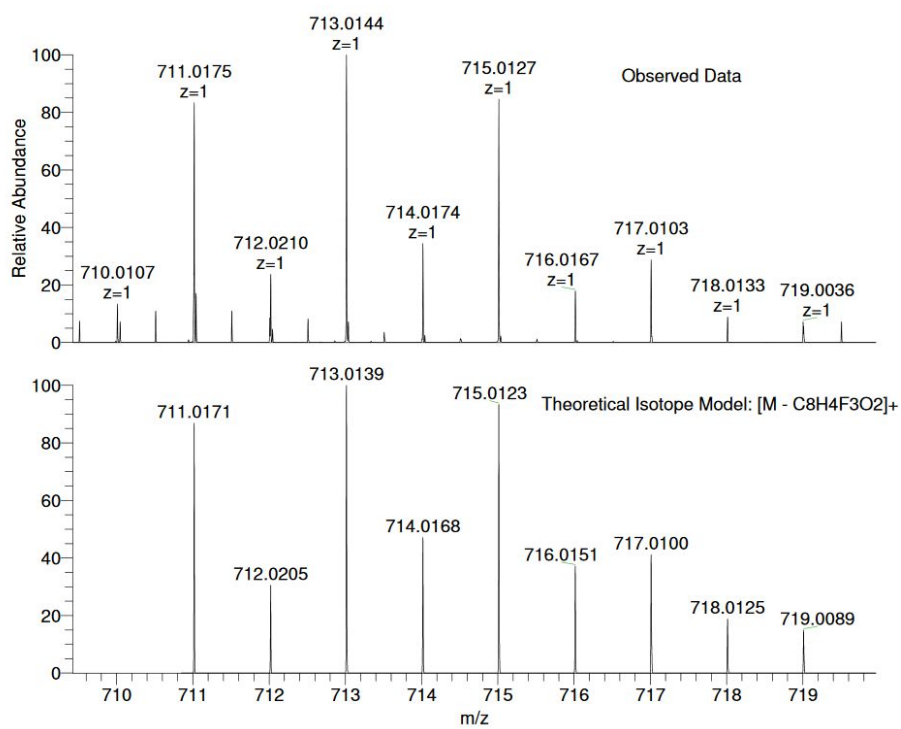
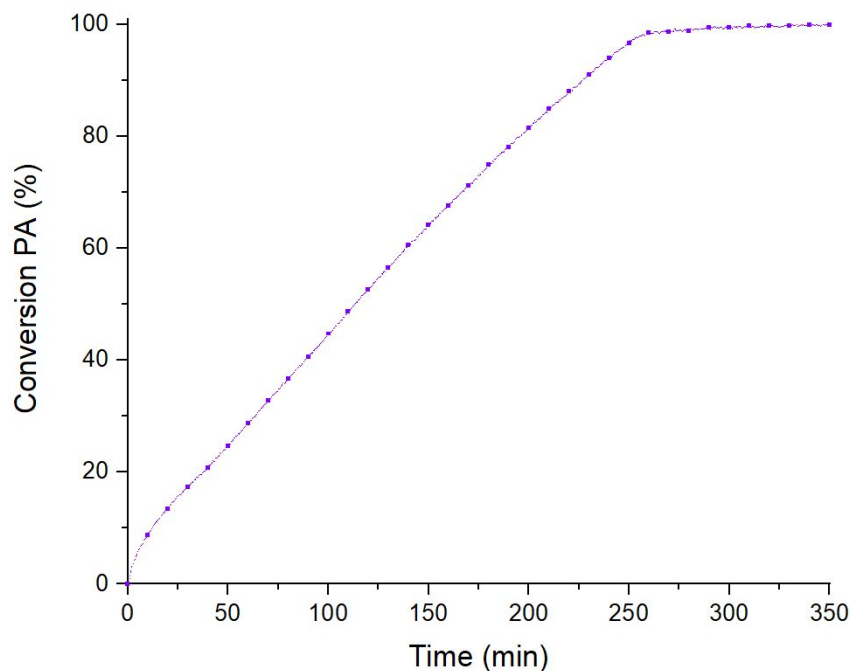
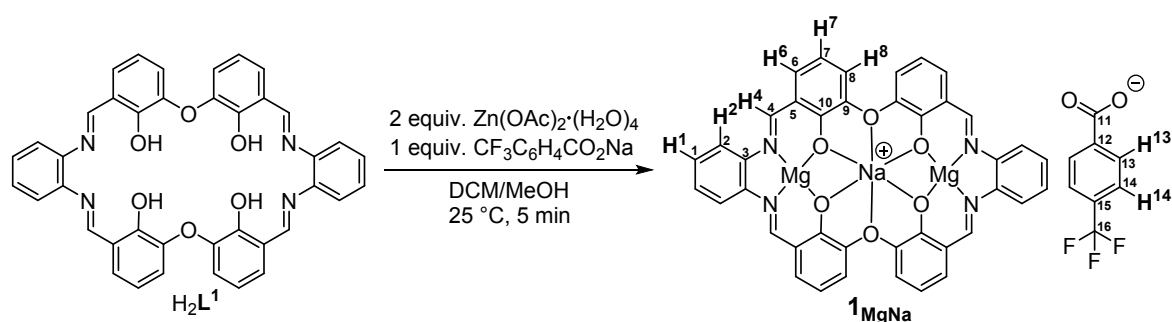


Figure S 45: Positive mode high-resolution ESI mass spectrum of  $6_{\text{ZnNa}}$



**Figure S 46:** Plot showing conversion of PA and CHO to PCHPE vs. time (Table S 2, run #6). Data are obtained using *in situ* ATR-IR spectroscopic monitoring of polymerizations conducted using 1 equiv.  $\mathbf{6}_{\text{ZnNa}}$ , 20 equiv. cyclohexane diol (CHD), 200 eqiv PA, 4000 equiv. cyclohexene oxide (CHO) and 1 bar  $\text{N}_2$  pressure at 100 °C. The conversion data was obtained by monitoring the changes to absorptions at 1730  $\text{cm}^{-1}$  (PCHC). The turn-over-frequency was obtained from 20-80.0% PA conversion.

### Section S8: Synthesis, characterisation and polymerisation kinetics of $\mathbf{1}_{\text{MgNa}}$



**Scheme S 11:** Synthesis of  $\mathbf{1}_{\text{MgNa}}$  from  $\text{H}_2\text{L}^1$  and NMR assignment numbering for  $\mathbf{1}_{\text{MgNa}}$ .

**Synthesis of  $\mathbf{1}_{\text{MgNa}}$ :** A solution of  $\text{Mg}(\text{OAc})_2 \cdot (\text{H}_2\text{O})_4$  (32.4 mg, 151  $\mu\text{mol}$ , 2 equiv.) and  $\text{CF}_3\text{C}_6\text{H}_4\text{CO}_2\text{Na}$  (17.2 mg, 75  $\mu\text{mol}$ , 1 equiv.) in MeOH (5 mL) was added to a solution of  $\text{H}_2\text{L}^1$  (50.0 mg, 75  $\mu\text{mol}$ , 1 equiv.) in 5 mL DCM (5 mL). The resulting solution was stirred for 5 min. Afterwards all volatiles were removed *in vacuo*, yielding a semi-solid which was washed with  $\text{Et}_2\text{O}$  (100 mL). To remove the acetic acid by-product fully, the

crude product was suspended in toluene (20 mL) which was afterwards removed under vacuum. This process was repeated, yielding  $1_{\text{MgNa}} \cdot 3\text{H}_2\text{O}$  as an orange powder (69.9 mg, 72  $\mu\text{mol}$ , 96%).

$^1\text{H}$  NMR (500 MHz,  $d_6$ -DMSO)  $\delta$  8.75 (s, 1H, H4), 7.87 (s, 0.5H, H13), 7.72 (dd,  $J$  = 6.1, 3.4 Hz, 1H, H2), 7.54 (s, 0.5H, H14), 7.39 (dd,  $J$  = 6.0, 3.3 Hz, 1H, H1), 7.23 (dd,  $J$  = 8.1, 1.8 Hz, 1H, H6), 7.10 (dd,  $J$  = 7.6, 1.9 Hz, 1H, H8), 6.50 (t,  $J$  = 7.7 Hz, 1H, H7).

$^{13}\text{C}$  NMR (126 MHz,  $d_6$ -DMSO)  $\delta$  172.76 (C11), 163.54 (C4), 161.31 (C5), 148.43 (C9), 142.62 (C3), 141.97 (C12), 129.99-129.57 (C6, C9, C13), 127.48 (C1), 124.33 (C14), 124.32 (q,  $J$  = 272.3 Hz, C16), 122.36 (C8), 120.46 (C15), 117.31 (C2), 111.40 (C7).

Elemental Analysis ( $1_{\text{MgNa}} \cdot 3\text{H}_2\text{O}$ ,  $\text{C}_{48}\text{H}_{28}\text{F}_3\text{Mg}_2\text{N}_4\text{NaO}_8$ ) calculated C 59.3% H 3.5% N 5.8% found C 59.3% H 3.4% N 5.9%

$^{19}\text{F}$  NMR (377 MHz,  $d_6$ -DMSO)  $\delta$  -60.97.

HRESI-MS  $m/z$  = calculated  $[\text{M} - \text{CF}_3\text{C}_6\text{F}_4\text{CO}_2]^+$  727.1289; found 727.1284.

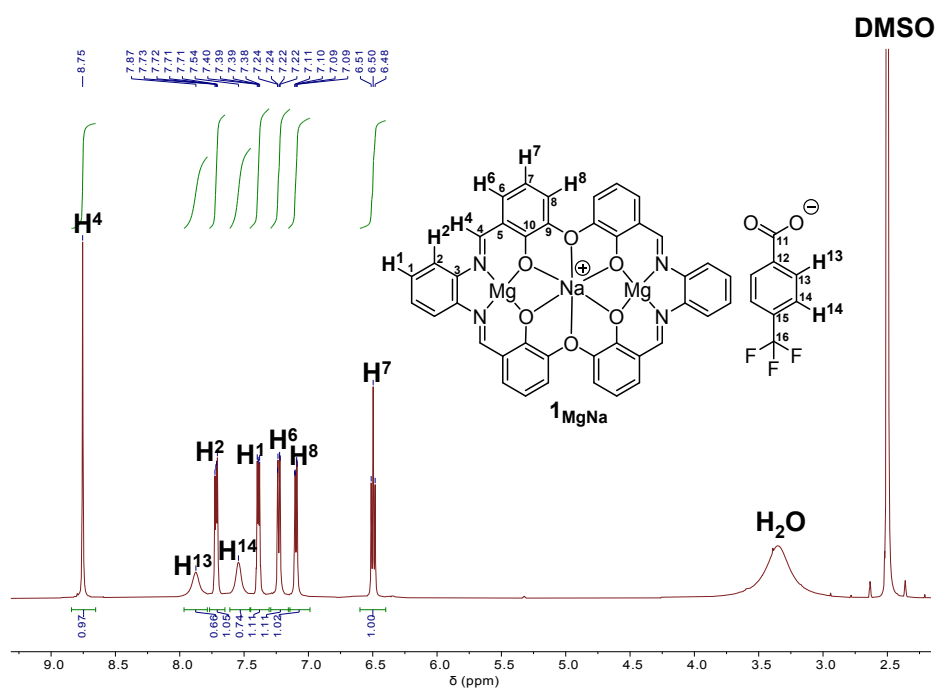


Figure S 47:  $^1\text{H}$  NMR spectrum (400 MHz,  $d_6$ -DMSO, 25°C) of  $1_{\text{MgNa}}$ .

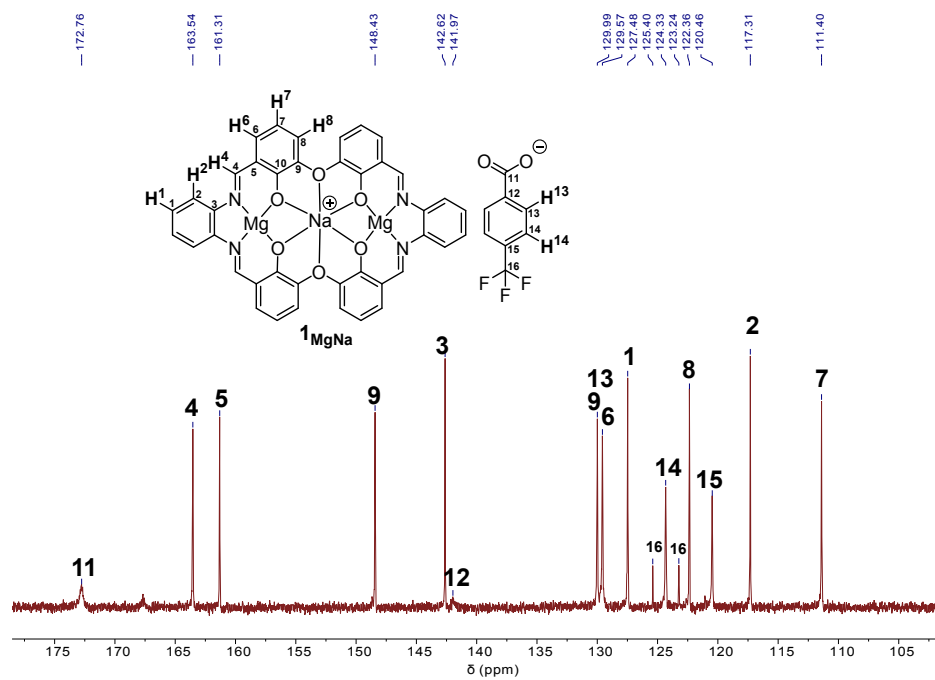


Figure S 48:  $^{13}\text{C}\{^1\text{H}\}$  NMR spectrum (126 MHz,  $\text{d}_6\text{-DMSO}$ ,  $25^\circ\text{C}$ ) of  $1_{\text{MgNa}}$ .

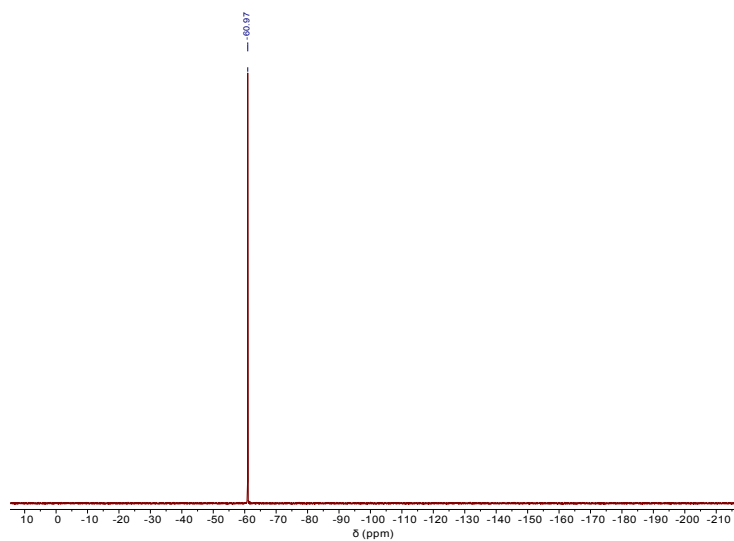
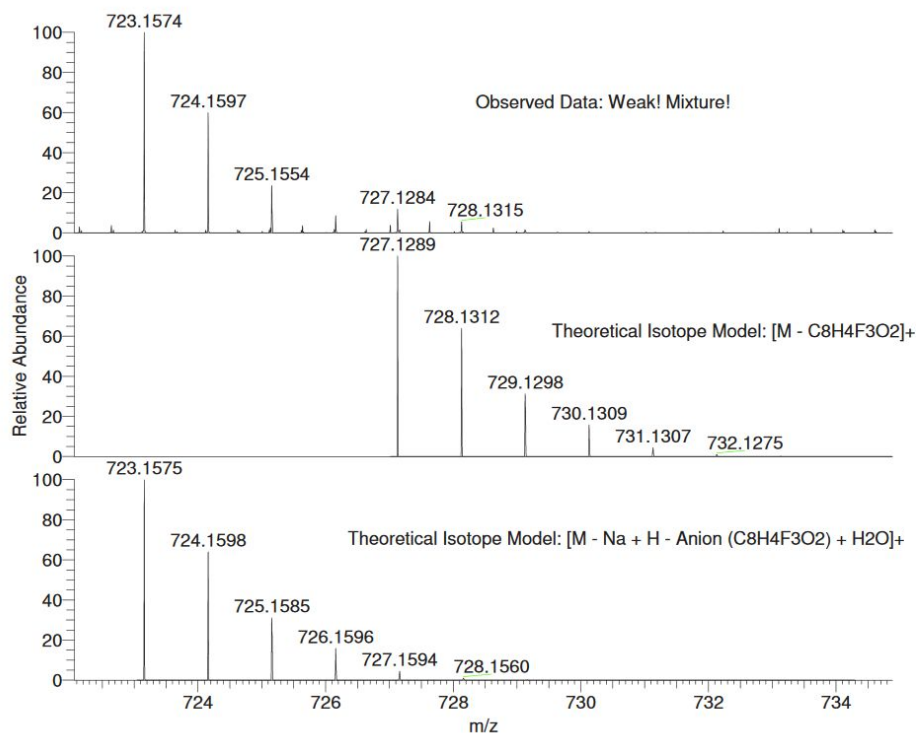
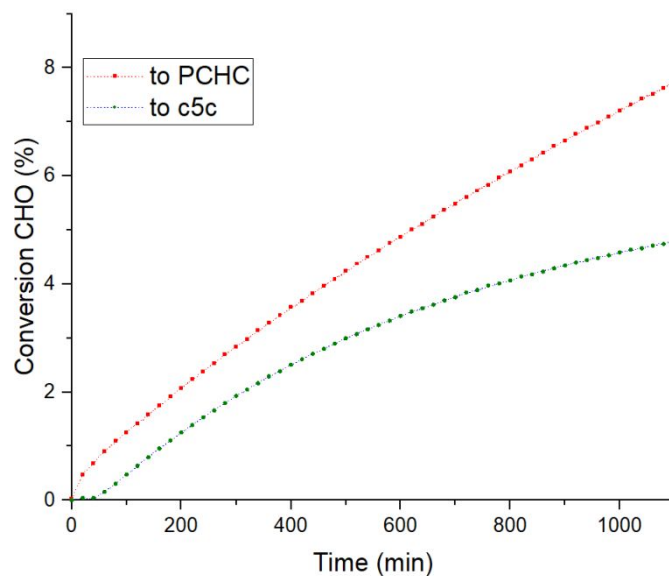


Figure S 49:  $^{19}\text{F}\{^1\text{H}\}$  NMR (377 MHz,  $\text{d}_6\text{-DMSO}$ ,  $25^\circ\text{C}$ ) of  $1_{\text{MgNa}}$ .



**Figure S 50:** Positive mode high-resolution ESI mass spectrum of  $1_{\text{MgNa}}$



**Figure S 51:** Plot showing conversion of CHO to polymer (PCHC) and c5c vs. time ( **Table S 1**, run #7). Data are obtained using *in situ* ATR-IR spectroscopic monitoring of polymerizations conducted using 1 equiv.  $1_{\text{MgNa}}$ , 20 equiv. cyclohexane diol (CHD), 4000 equiv. cyclohexene oxide (CHO) and 1 bar carbon dioxide pressure at 100 °C. The conversion data was obtained by monitoring the changes to absorptions at 1744  $\text{cm}^{-1}$  (PCHC) and 1785  $\text{cm}^{-1}$  (c5c). The turn-over-frequency (TOF = 16  $\text{h}^{-1}$ ) was obtained from 1-8.0% conversion to PCHC.

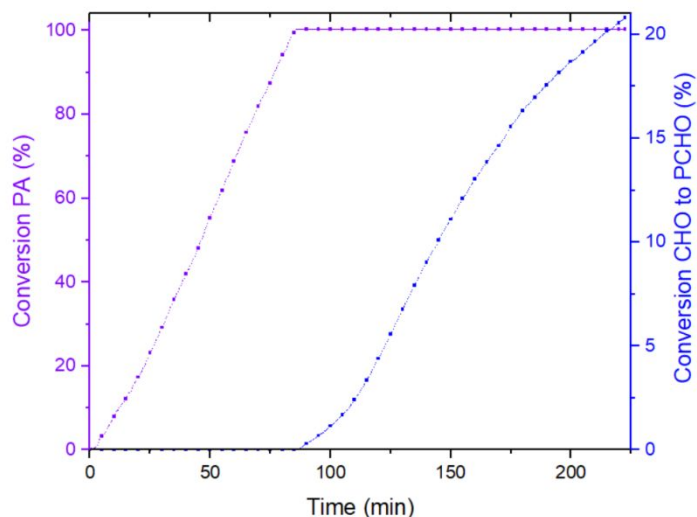


**Figure S 52:** Plot showing conversion of PA and CHO to polymer (PCHPE and PCHO respectively) vs. time (**Table S 2**, run #7). Data are obtained using *in situ* ATR-IR spectroscopic monitoring of polymerizations conducted using 1 equiv. **1**<sub>MgNa</sub>, 20 equiv. cyclohexane diol (CHD), 200 eqiv PA, 4000 equiv. cyclohexene oxide (CHO) and 1 bar N<sub>2</sub> pressure at 100 °C. The conversion data was obtained by monitoring the changes to absorptions at 1730 cm<sup>-1</sup> (PCHPE) and 1089 cm<sup>-1</sup> (PCHO). The turn-over-frequency was obtained from 20-80.0% PA conversion.

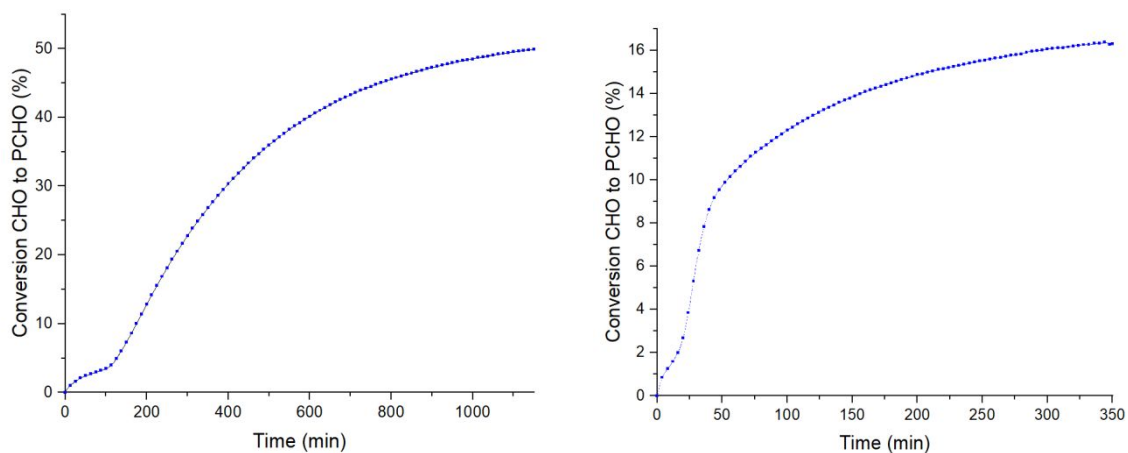
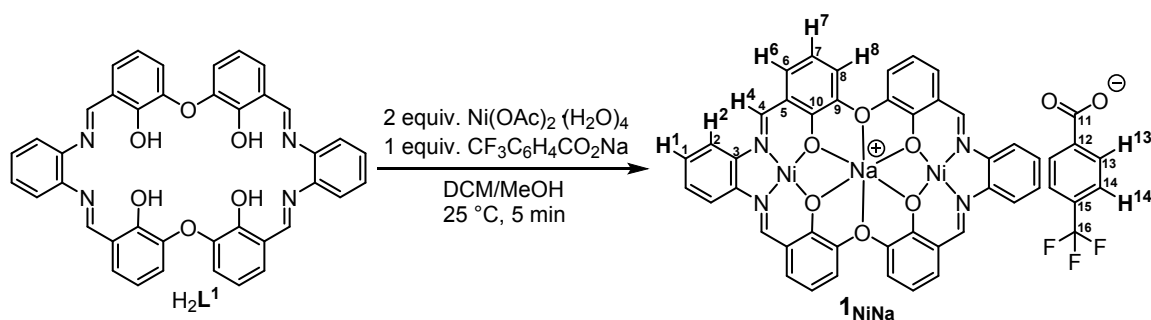


**Figure S 53:** Plots showing conversion of homopolymerisation of CHO (1 equiv. cat, 20 equiv. CHD, 4000 equiv. CHO, 100°C) with (left) **1**<sub>MgNa</sub> and (right) **1**<sub>ZnNa</sub> showing that overall CHO conversion is intrinsically pseudo equilibrium limited at different monomer conversions.

## Section S9: Synthesis, characterisation and polymerisation kinetics of $1_{\text{NiNa}}$



**Scheme S 12:** Synthesis of  $1_{\text{NiNa}}$  from  $\text{H}_2\text{L}^1$  and NMR assignment numbering for  $1_{\text{NiNa}}$ .

**Synthesis of  $1_{\text{MgNa}}$ :** A solution of  $\text{Ni}(\text{OAc})_2 \cdot (\text{H}_2\text{O})_4$  (37.5 mg, 151  $\mu\text{mol}$ , 2 equiv.) and  $\text{CF}_3\text{C}_6\text{H}_4\text{CO}_2\text{Na}$  (17.2 mg, 75  $\mu\text{mol}$ ) in MeOH (5 mL, 1 equiv.) was added to a solution of  $\text{H}_2\text{L}^1$  (50.0 mg, 75  $\mu\text{mol}$ , 1 equiv.) in 5 mL DCM (5 mL). The resulting solution was stirred for 5 min. Afterwards all volatiles were removed *in vacuo*, yielding a semi-solid which was washed with  $\text{Et}_2\text{O}$  (100 mL). To remove the acetic acid by-product fully, the crude product was suspended in toluene (20 mL) which was afterwards removed under vacuum. This process was repeated, yielding  $1_{\text{NiNa}} \cdot 2\text{H}_2\text{O}$  as a orange powder (71.2 mg, 71  $\mu\text{mol}$ , 94%).

**$^1\text{H}$  NMR (500 MHz,  $d_6$ -DMSO)**  $\delta$  9.54 (s, 1H, H4), 8.26 (dd,  $J$  = 6.5, 3.4 Hz, 1H, H2), 8.08 (s, 0.5H, H13), 7.67 (s, 0.5H, H14), 7.55 – 7.48 (m, 2H, H6, H1), 7.45 (d,  $J$  = 7.4 Hz, 1H, H8), 6.80 (t,  $J$  = 7.9 Hz, 3H, H7).

No  $^{13}\text{C}$  spectrum could be obtained due to the low solubility of  $1_{\text{NiNa}}$  in all common organic solvents.

**Elemental Analysis ( $1_{\text{NiNa}} \cdot 2\text{H}_2\text{O}$ ,  $\text{C}_{48}\text{H}_{32}\text{F}_3\text{Ni}_2\text{N}_4\text{NaO}_{10}$ )** calculated C 57.4% H 3.0% N 5.6% found C 57.2% H 3.4% N 5.6%

**$^{19}\text{F}$  NMR (377 MHz, DMSO)**  $\delta$  -60.99 ( $\text{CF}_3$ ).

**HRESI-MS  $m/z$**  = calculated  $[\text{M} - \text{CF}_3\text{C}_6\text{H}_4\text{CO}_2\text{Na}]^+$  795.0295; found 795.0295.

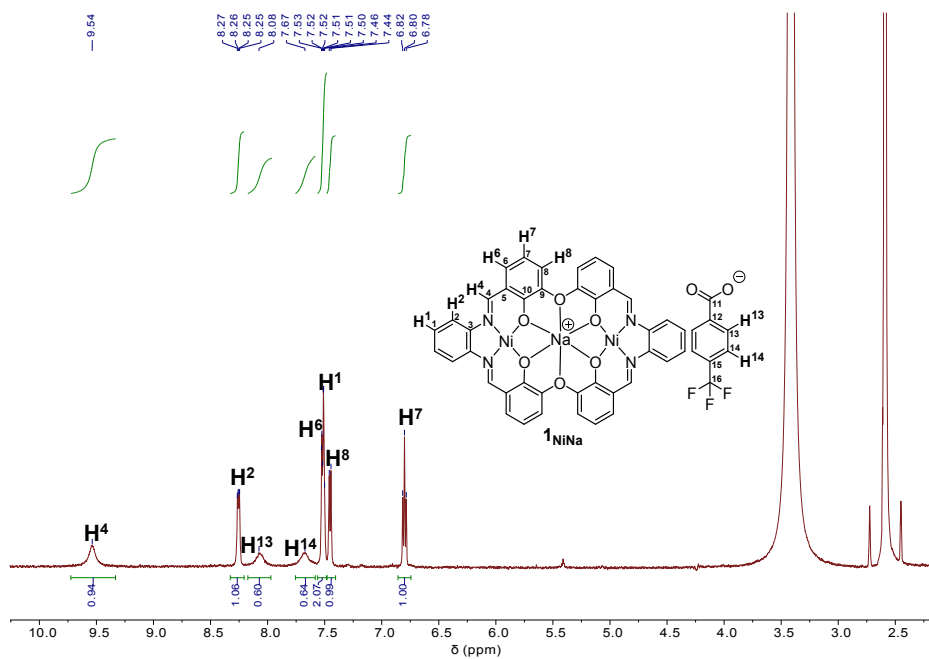


**Figure S 54:**  $^1\text{H}$  NMR spectrum (400 MHz,  $\text{d}_6\text{-DMSO}$ ,  $25^\circ\text{C}$ ) of **1NiNa**.

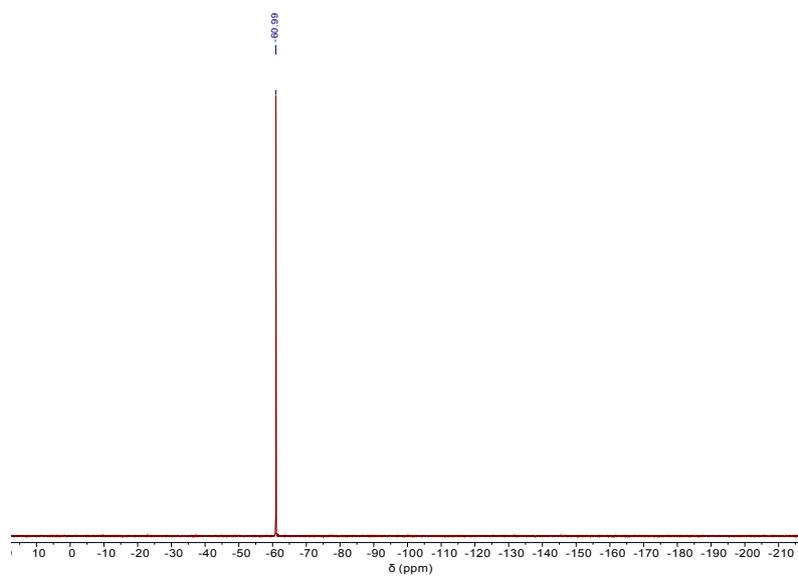


**Figure S 55:**  $^{19}\text{F}\{^1\text{H}\}$  NMR (377 MHz,  $\text{d}_6\text{-DMSO}$ ,  $25^\circ\text{C}$ ) of **1NiNa**.

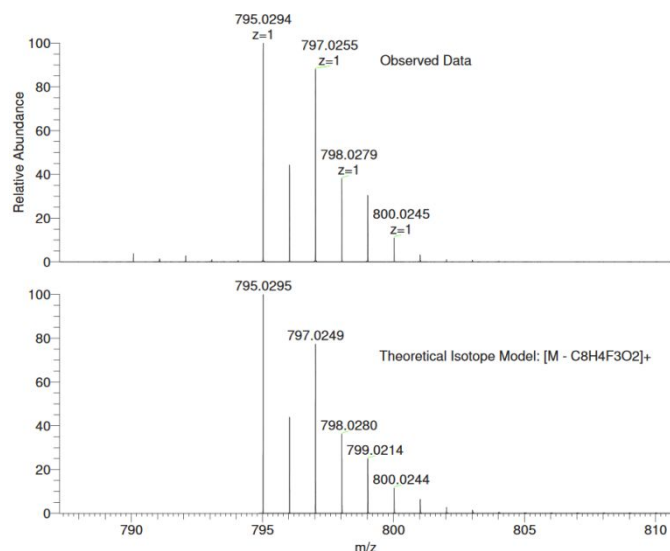


**Figure S 56:** Positive mode high-resolution ESI mass spectrum of  $1_{NiNa}$

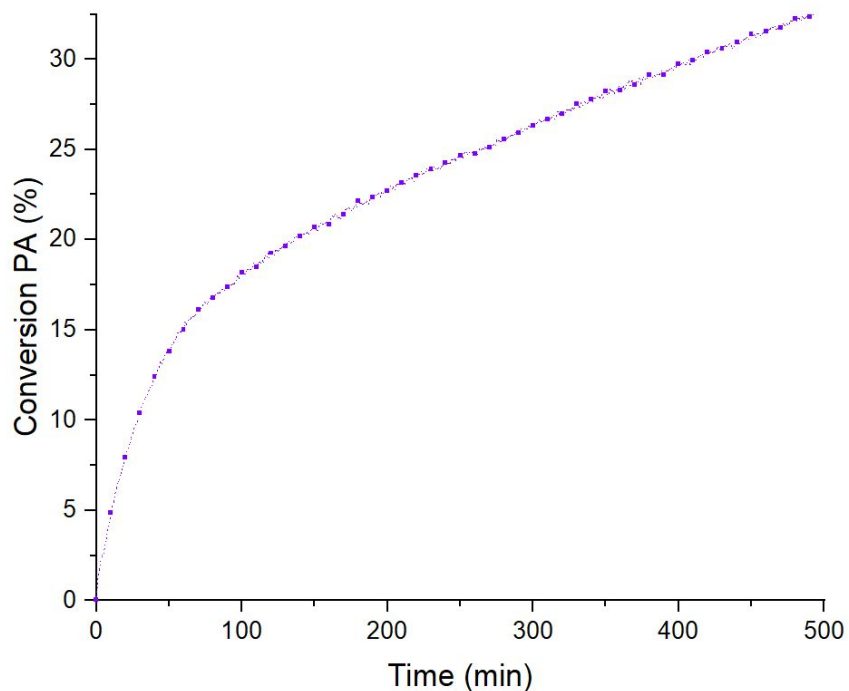
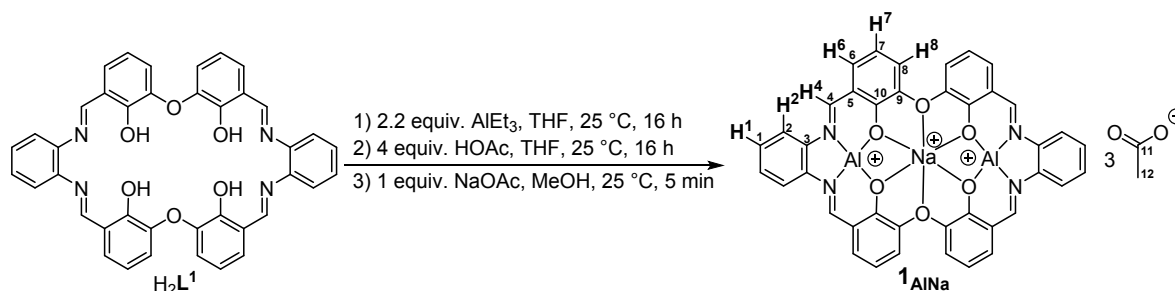


**Figure S 57:** Plot showing conversion of PA and CHO to polymer (PCHPE) vs. time (Table S 2, run #8). Data are obtained using *in situ* ATR-IR spectroscopic monitoring of polymerizations conducted using 1 equiv.  $1_{NiNa}$ , 20 equiv. cyclohexane diol (CHD), 200 equiv PA, 4000 equiv. cyclohexene oxide (CHO) and 1 bar  $N_2$  pressure at 100 °. Decrease in activity occurs together with precipitation of a solid.

## Section S10: Synthesis, characterisation and polymerisation kinetics of $1_{\text{AlNa}}$



**Scheme S 13:** Synthesis of  $1_{\text{AlNa}}$  from  $\text{H}_2\text{L}^1$  and NMR assignment numbering for  $1_{\text{AlNa}}$ .

**Synthesis of  $1_{\text{AlNa}}$ :**  $\text{AlEt}_3$  (18.8 mg, 165  $\mu\text{mol}$ , 2.2 equiv.) was added to a solution of  $\text{H}_2\text{L}^1$  (50.0 mg, 75  $\mu\text{mol}$ , 1 equiv.) in 5 mL THF (5mL). The resulting solution was stirred overnight at room temperature. Afterwards glacial acetic acid (14.9 mg, 248  $\mu\text{mol}$ , 3.3 equiv.) was added and the resulting mixture was stirred for 5h during which a yellow solid precipitated which was isolated by centrifugation. The solid was dissolved in MeOH (5 mL) and NaOAc (6.2 mg, 75  $\mu\text{mol}$ , 1 equiv.) was added. The resulting solution was added to  $\text{Et}_2\text{O}$  (100 mL) leading to the precipitation of a yellow solid. Precipitation from MeOH/ $\text{Et}_2\text{O}$  was repeat another two times. Isolation by centrifugation and drying *in vacuo* yielded  $1_{\text{AlNa}}$  as a yellow powder (31.5 mg, 35  $\mu\text{mol}$ , 46% yield).

**$^1\text{H}$  NMR (500 MHz,  $\text{d}_4\text{-MeOH}$ )**  $\delta$  9.15 (s, 1H, H4), 8.02 (dd,  $J = 6.1, 3.3$  Hz, 1H, H2), 7.62 (dd,  $J = 6.1, 3.2$  Hz, 1H, H1), 7.45-7.45 (m, 2H, H6, H8), 6.84 (t,  $J = 7.9$  Hz, 1H, H7), 1.74 (s, 3H, H12).

**$^{13}\text{C}$  NMR (126 MHz,  $\text{d}_4\text{-MeOH}$ )**  $\delta$  178.97 (C11), 163.52 (C4), 158.16 (C10), 147.81 (C9), 139.92 (C3), 130.68 (C1), 130.22 (C8), 123.02 (C6), 122.59 (C5), 118.29 (C2), 117.01 (C7), 23.44 (C12).

No suitable elemental analysis could be obtained

**HRESI-MS  $m/z$**  = calculated  $[\text{M} - \text{OAc}]^+$  851.1485; found 851.1488.

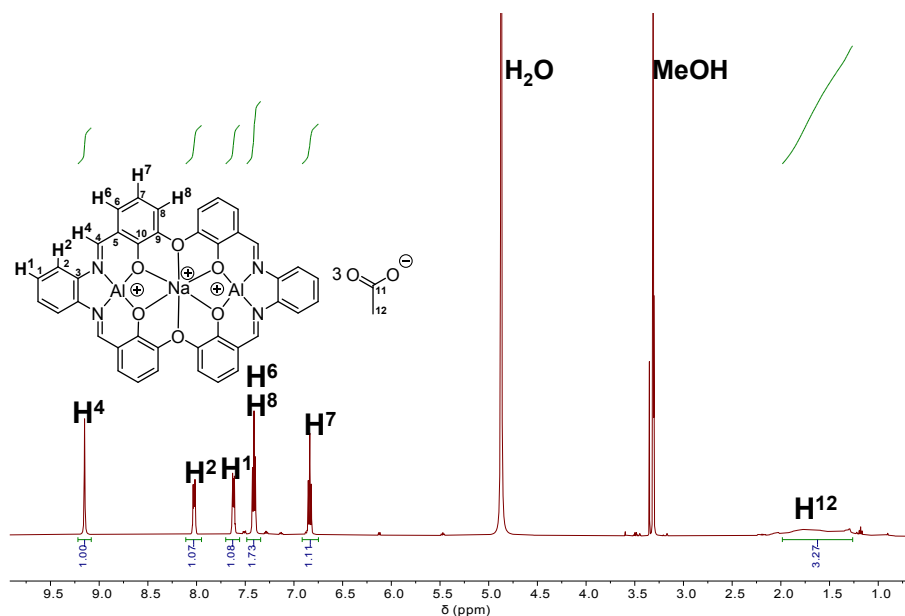


Figure S 58:  $^1H$  NMR spectrum (500 MHz,  $d_4$ -MeOH, 25°C) of  $1_{AlNa}$ .

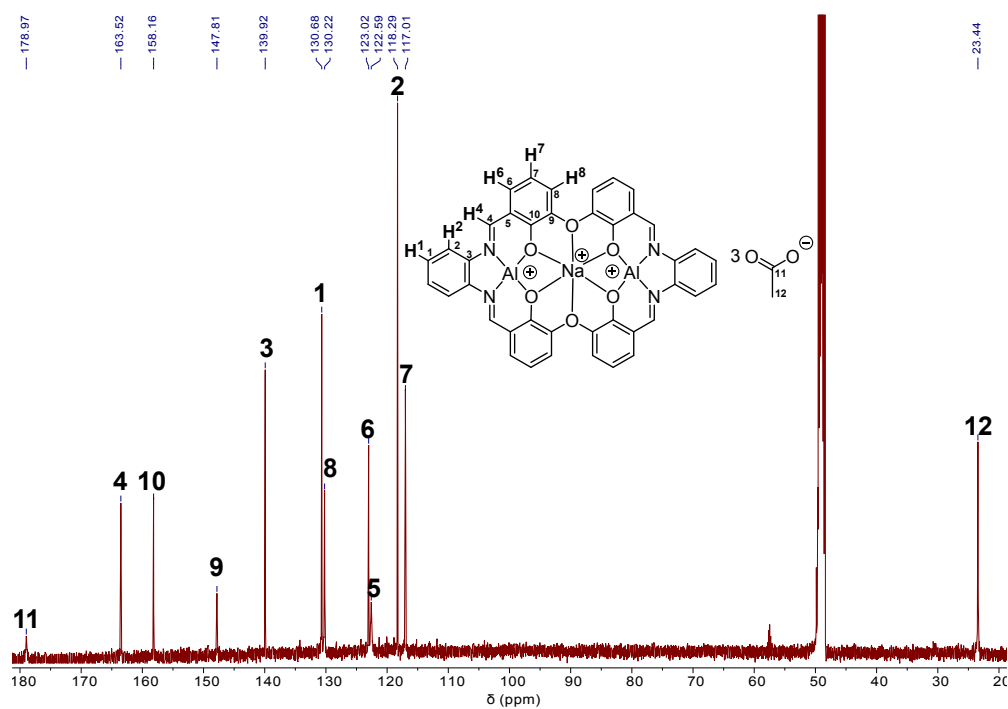
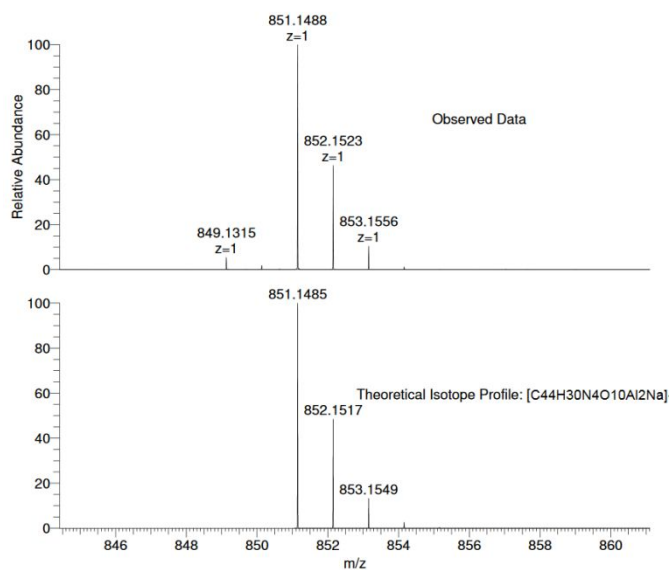
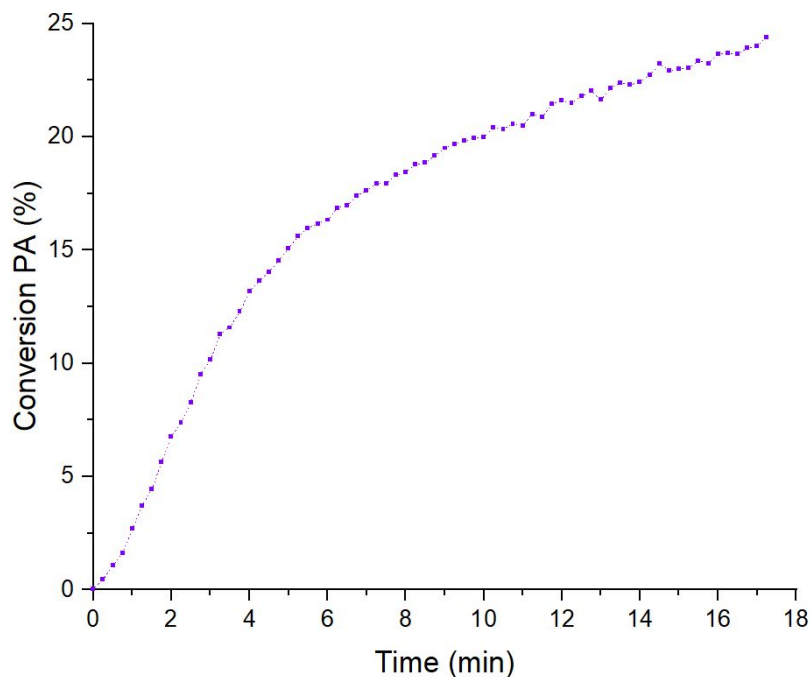


Figure S 59:  $^{13}C\{^1H\}$  NMR spectrum (126 MHz,  $d_4$ -MeOH, 25°C) of  $1_{AlNa}$ .

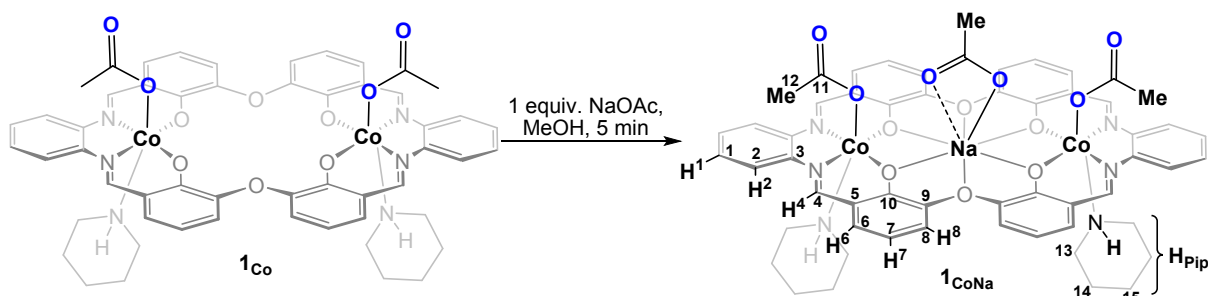


**Figure S 60:** Positive mode high-resolution ESI mass spectrum of  $1_{AlNa}$



**Figure S 61:** Plot showing conversion of PA and CHO to polymer (PCHPE) vs. time (Table S 2, run #9). Data are obtained using *in situ* ATR-IR spectroscopic monitoring of polymerizations conducted using 1 equiv.  $1_{AlNa}$ , 20 equiv. cyclohexane diol (CHD), 200 equiv PA, 4000 equiv. cyclohexene oxide (CHO) and 1 bar  $N_2$  pressure at 100 °. Decrease in activity occurs together with emergence of a colour change of yellow to deep red.

## Section S11: Synthesis, characterisation and polymerisation kinetics of $1_{\text{CoNa}}$



**Scheme S2:** Synthesis of  $1_{\text{CoNa}}$  from  $1_{\text{Co}}$  and NMR assignment numbering for  $1_{\text{CoNa}}$ .

**Synthesis of  $1_{\text{CoNa}}$ :**  $1_{\text{Co}}$  (30.0 mg, 27  $\mu\text{mol}$ , 1 equiv.) and NaOAc (2.3 mg, 27  $\mu\text{mol}$ , 1 equiv.) are dissolved in MeOH (0.7 mL). After 1 min the solvent was removed under stream of nitrogen and the resulting solid was taken up in 0.7 mL  $d_6$ -DMSO and analysed by  $^1\text{H}$  NMR spectroscopy. Due to the instability of  $1_{\text{CoNa}}$  no further analysis could be obtained.

Note that in order to employ  $1_{\text{CoNa}}$  in polymerisation the complex was prepared in the polymerisation tube in MeOH which was removed in vacuo prior to addition of CHO, CHD and  $\text{CO}_2$ .

**$^1\text{H}$  NMR (400 MHz,  $d_6$ -DMSO):**  $\delta$  8.63 (s, 4H, H3), 8.27 (dd,  $J = 6.2, 3.4$  Hz, 4H, H2), 7.59 (dd,  $J = 6.2, 3.2$  Hz, 4H, H1), 7.34 (dd,  $J = 8.1, 1.7$  Hz, 4H, H6), 7.19 (dd,  $J = 7.7, 1.7$  Hz, 4H, H8), 6.61 (t,  $J = 7.8$  Hz, 4H, H7), 4.80 – 4.52 (t,  $J = 9.0$  Hz, 2H), 2.43 (d,  $J = 11.2$  Hz, 4H,  $\text{H}_{\text{Pip}}$ ), 1.70 – 0.75 (m, 25H,  $\text{H}_{\text{Pip}}$ /Me).

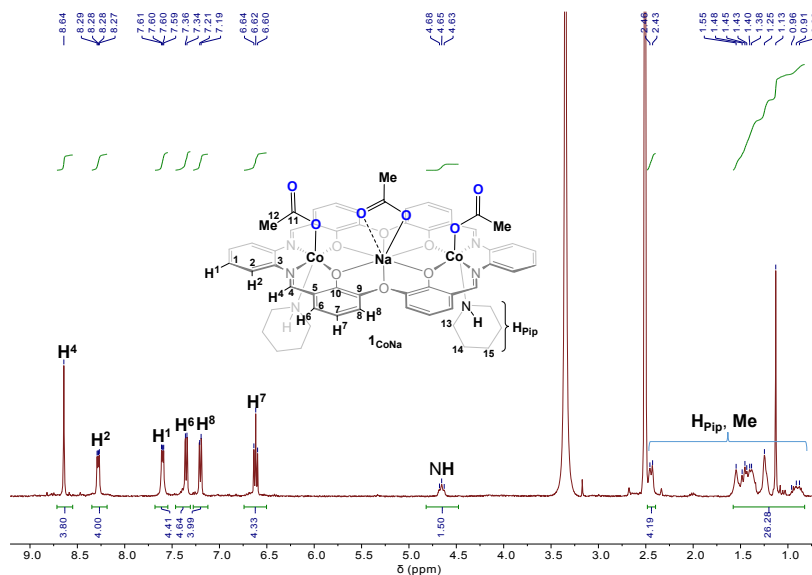


**Figure S 62:**  $^1\text{H}$  NMR spectrum (400 MHz,  $d_6$ -DMSO, 25°C) of  $1_{\text{CoNa}}$ .

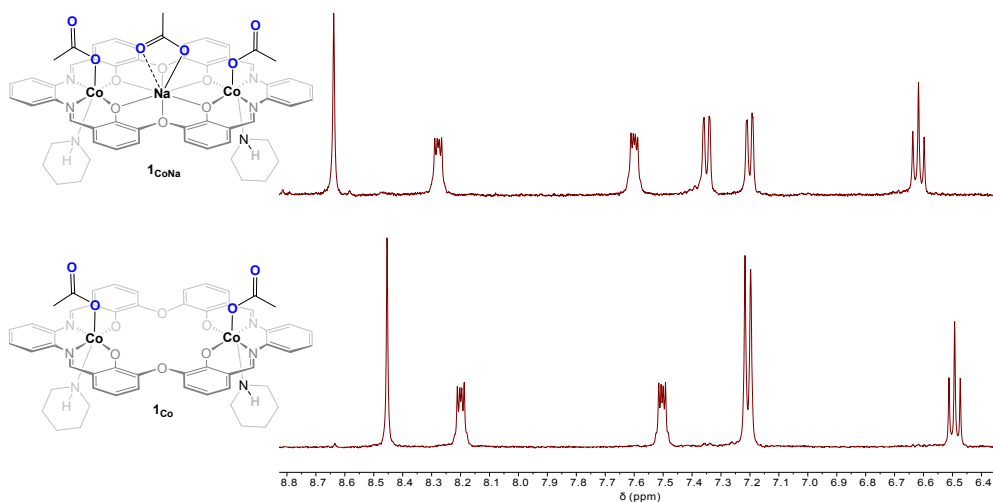


**Figure S 63:**  $^1\text{H}$  NMR spectrum (400 MHz,  $d_6$ -DMSO, 25°C) of  $1_{\text{CoNa}}$ .

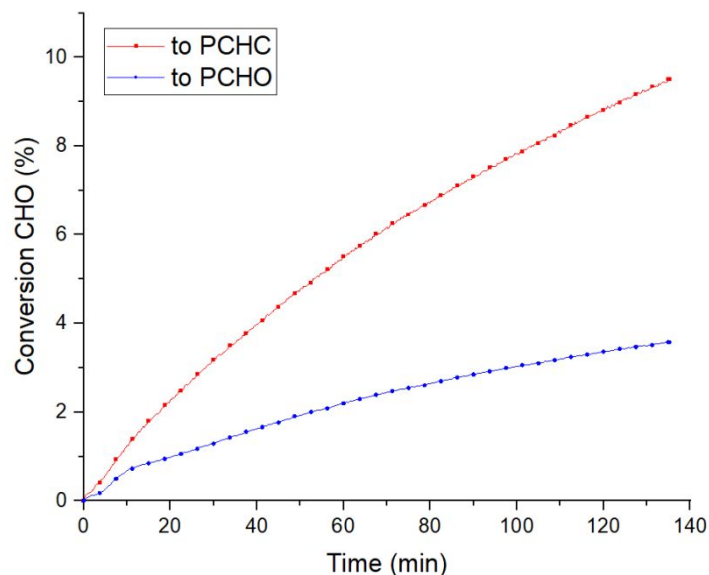


**Figure S 64:** Plot showing conversion of CHO to polymer (PCHC) and c5c vs. time (

**Table S 1**, run #10). Data are obtained using *in situ* ATR-IR spectroscopic monitoring of polymerizations conducted using 1 equiv.  $1_{\text{MgNa}}$ , 20 equiv. cyclohexane diol (CHD), 4000 equiv. cyclohexene oxide (CHO) and 1 bar carbon dioxide pressure at 100 °C. The conversion data was obtained by monitoring the changes to absorptions at 1744  $\text{cm}^{-1}$  (PCHC) and 1785  $\text{cm}^{-1}$  (c5c). The turn-over-frequency (TOF) were obtained from 0-10% conversion to polymer.

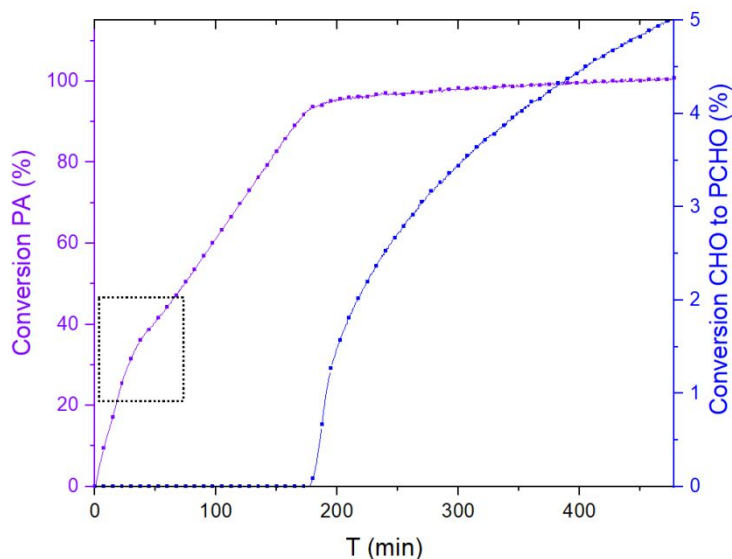


**Figure S 65:** Plot showing conversion of PA and CHO to polymer (PCHPE) vs. time (**Table S 2**, run #10). Data are obtained using *in situ* ATR-IR spectroscopic monitoring of polymerizations conducted using 1 equiv.  $1_{\text{CoNa}}$ , 20 equiv. cyclohexane diol (CHD), 200 eqiv PA, 4000 equiv. cyclohexene oxide (CHO) and 1 bar  $\text{N}_2$  pressure at  $80^\circ\text{C}$  (**Table S 2**, run #10). Change in activity (highlighted by dotted box) is inferred to be a consequence of Co(III) to Co(II) thermal reduction. The turn-over-frequency (TOF) were obtained from 0-30% and 40-90% PA conversion.

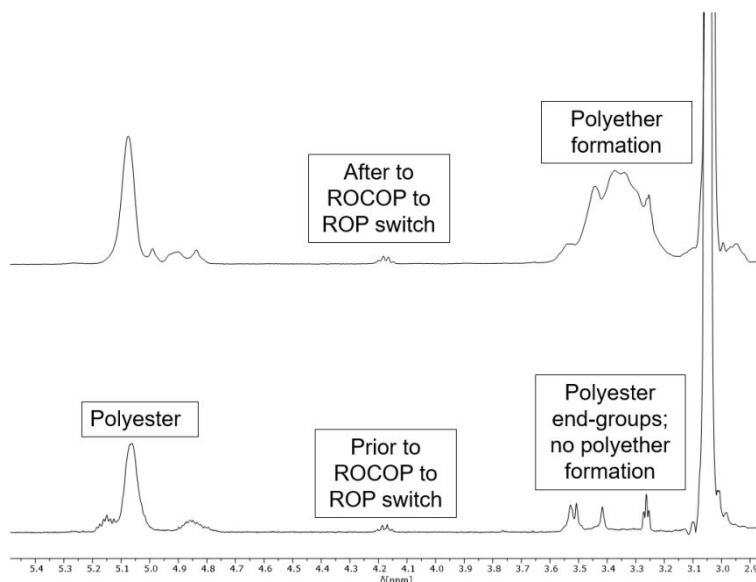


**Figure S 66:** Stacked  $^1\text{H}$  NMR spectra (400 MHz,  $\text{CDCl}_3$ ,  $25^\circ\text{C}$ ) of aliquots removed prior and after ROCOP to ROP switch (corresponding to **Figure S 52**) showing ether linkage formation exclusively occurs after mechanistic switch.

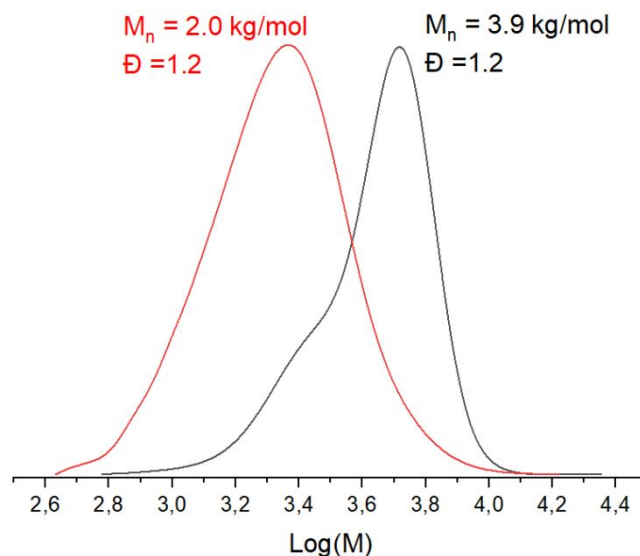


**Figure S 66:** Stacked GPC traces of aliquots removed prior and after ROCOP to ROP switch (corresponding to **Figure S 52**) showing growth of formed polymer chains after mechanistic switch rather than generation of new chains. Furthermore polymer samples maintain composition through multiple precipitation from DCM/MeOH or DCM/pentane further confirming block connection.

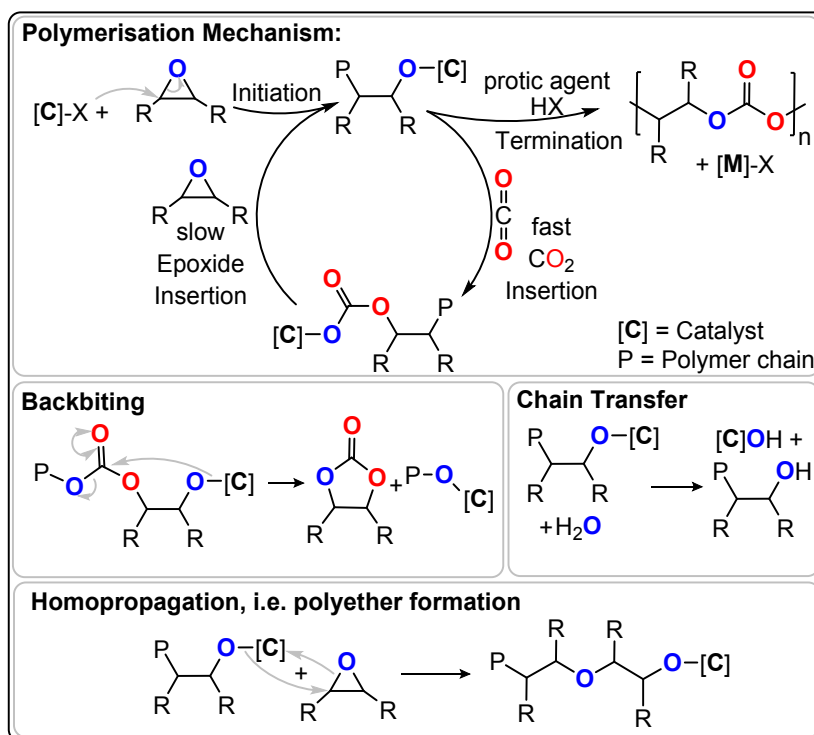


**Figure S 67:** Example ROCOP mechanism for  $\text{CO}_2$ /epoxide copolymerisation.

- [1] Akine, S.; Utsuno, F.; Piao, S.; Orita, H.; Tsuzuki, S.; Nabeshima, T. Synthesis, Ion Recognition Ability, and Metal-Assisted Aggregation Behavior of Dinuclear Metallohosts Having a Bis(Saloph) Macrocyclic Ligand. *Inorg. Chem.* **2016**, *55* (2), 810–821.
- [2] Sakata, Y.; Okada, M.; Tamiya, M.; Akine, S. Post-Metalation Modification of a Macrocyclic Dicobalt(III) Metallohost by Site-Selective Ligand Exchange for Guest Recognition Control. *Chem. Eur. J.* **2020**, *26* (34), 7595–7601
- [3] Plajer, A. J.; Williams, C. K. Heterotrimetallic Carbon Dioxide Copolymerization and Switchable Catalysts: Sodium Is the Key to High Activity and Unusual Selectivity. *Angew. Chem. Int. Ed.* **2021**, *60* (24), 13372–13379